



LAWRENCE
LIVERMORE
NATIONAL
LABORATORY

Comparison of DOTC and Legacy Benziger Dry Aminated TATBs and PBX-9502

D. M. Hoffman, A. Martin-Williams, F. J. Gagliardi,
T. K. Lorenz, T. Willley, T. D. Tran

June 26, 2013

NDIA Insensitive Munitions and Energetic Materials
Technology Symposium
San Diego, CA, United States
October 7, 2013 through October 10, 2013

Disclaimer

This document was prepared as an account of work sponsored by an agency of the United States government. Neither the United States government nor Lawrence Livermore National Security, LLC, nor any of their employees makes any warranty, expressed or implied, or assumes any legal liability or responsibility for the accuracy, completeness, or usefulness of any information, apparatus, product, or process disclosed, or represents that its use would not infringe privately owned rights. Reference herein to any specific commercial product, process, or service by trade name, trademark, manufacturer, or otherwise does not necessarily constitute or imply its endorsement, recommendation, or favoring by the United States government or Lawrence Livermore National Security, LLC. The views and opinions of authors expressed herein do not necessarily state or reflect those of the United States government or Lawrence Livermore National Security, LLC, and shall not be used for advertising or product endorsement purposes.

Comparison of DOTC and Legacy Benziger Dry Aminated TATBs and PBX-9502†

D. Mark Hoffman*, Audrey Martin-Williams, Franco Gagliardi, Thomas K. Lorenz, Trevor Willey and Tri D. Tran

High Explosives Application Facility
Physical and Life Sciences Division
Lawrence Livermore Laboratory, Livermore, CA

Abstract

As part of a Defense Department Ordnance Technology Consortium (DOTC) effort, Lab and pilot scale batches of dry aminated 1,3,5-triamino-2,4,6-trinitrobenzene (DA TATB) synthesized by ATK and BAE were characterized and compared to legacy dry aminated TATB produced in the late 1980's. Among the techniques for characterizing the new TATB were small scale safety tests (drop hammer, friction, spark, chemical reactivity (CRT) and differential scanning calorimetry (DSC), particle size distribution by laser light scattering, void distribution by ultra-small angle x-ray scattering (USAXS), morphology by optical microscopy (OM) and scanning electron microscopy (SEM) and crystal softness by compression molding using a "Heckel" yield pressure (stress). Subsequently PBX-9502 molding powder was slurry coated from new TATBs. PBX-9502 is 95/5:DA TATB/Kel-F 800 polymer binder. New FK-800 was used in all PBXs instead of legacy Kel-F 800. PBX-9502 molding powder was compression molded into 1" by ½" diameter cylinders for evaluation of density and mechanical properties. Compressive mechanical properties were evaluated at -20, 23 and 50°C. Relative detonation energies and detonation velocities were evaluated using the new disc acceleration experiment (DAX) with piezoelectric pins and a photonic doppler velocimetry (PDV) gauge that measured an aluminum flyer foil's velocity. Although there were slight differences in these tests, the general conclusion was that the new DA TATBs were sufficiently similar to legacy material to be suitable replacements for any DOE requirements for DA TATB. This does not remove the necessity of evaluating explosives formulated from this material in future systems, but does show high probability of success using the new DA TATBs as a replacement for legacy TATB in PBXs and weapons systems without compromising performance or safety.

*corresponding author hoffman2@llnl.gov

† This work performed under the auspices of the U.S. Department of Energy by Lawrence Livermore National Laboratory under Contract DE-AC52-07NA27344

Introduction:

Modern Department of Energy (DOE) weapons systems designed by LLNL use the insensitive high explosive 1,3,5-triamino-2,4,6-trinitrobenzene (TATB) synthesized by the Benziger process[1, 2] for reliability, enhanced safety and excellent aging characteristics. Unfortunately, no production quantities of DA TATB have been manufactured in the US by this route since the mid 1980's. Recently the Department of Defense (DoD) became interested in reduced sensitivity boosters such as PBXN-7 and PBXW-14. These formulations contain TATB. Since there was no source of production scale TATB, DOD launched a MANTECH TATB program to develop TATB based on two different synthetic routes[3, 4]. It has been shown that routes involving other halogens, alkoxy or vicarious nucleophilic substitution, at least at small scale, produce TATB with reduced thermal stability.[5] We evaluated these TATB's as possible replacements for our needs but found they were unsatisfactory. [6, 7] Recently as part of a Defense Department Ordnance Technology Consortium (DOTC) effort, lab and pilot scale batches of Benziger process dry aminated (DA) TATB were synthesized by Alliant Techsystems Inc. at Radford Army Ammunition Plant (ATK) and British Aerospace Engineering at Holston Army Ammunition Plant (BAE). As part of the process, DoD put together a team to evaluate the new DA TATBs from both vendors. This report describes some of the results generated by LLNL evaluating the DA TATB synthesized at the laboratory and pilot scales as part of the Joint DOD-DOE working group effort.

The DOE specification for TATB explosive crystals (13Y-188025) was written for TATB made by the Benziger synthesis route. This specification calls out a particular particle size, low impurity levels, color, foreign matter limits, etc. However, the current specification does not cover crystal quality or compaction characteristics of the powder and, of course, no properties of the plastic bonded explosives made from the TATB are included. The DOE uses TATB with Kel-F 800, a copolymer of vinylidene fluoride and chlorotrifluoroethylene, in weight ratios of 95/5 or 92.5/7.5 called PBX-9502 and LX-17, respectively. Recently 3M Corporation modified its Kel-F 800 production process and a new version of this polymer called FK-800 is now commercially available and was used.[8] A scaled down version of the slurry coating process used by BAE was used to prepare PBX-9502 from the new TATB samples so that it would resemble, as closely as possible, legacy PBX-9502. The new formulations were compared to legacy PBX-9502 and PBX-9502-like explosive made from legacy TATB at the 50 gram scale by evaluating pressing characteristics, mechanical properties in compression and detonation behavior.

Experimental:

A. Neat TATB Characterization

Small Scale Safety tests: Five small scale safety tests are performed on all LLNL explosives and formulations. These tests are Drop Hammer (DH 50), BAM friction, spark, differential scanning calorimetry (DSC) and chemical reactivity tests (CRT). These tests are described elsewhere. [9-12]

Morphology, particle size distribution and crystal quality: Morphological comparisons of the various TATBs were made using a LEO 438 VP (variable pressure) scanning electron microscope (SEM). The variable pressure SEM reduces surface charging of an organic sample by allowing a low pressure atmosphere to pass over the sample to bleed off excess charge. The morphology of TATBs was also evaluated using a Zeiss 40-A polarizing microscope under crossed polars with a first-order red plate.

Optical micrographs were calibrated with a stage micrometer at the same magnification with Zeiss Axiovision software. All optical micrographs are shown at approximately the same magnification for ease of comparison. Particle size distributions were measured using a Saturn DigiSizer 5200 laser light scattering apparatus manufactured by Micromeritics Instrument Corporation. Samples of approximately 60-80 mg of TATB in 2-mL DI water were dispersed with Coulter 1 A surfactant in 2-3 ml of DI water and 3 min of sonication in an external sonicator. Usually, although not always 3 measurements of each of two 2 TATB samples from a given lot were made and the average of the 3 runs were reported. A description of the procedures used with these tools can be found in the manufacture's users manuals.[13-15]

Ultra small angle x-ray scattering was used to evaluate defects in the new TATB crystal compared to legacy dry aminated TATB. Interstitial scattering was mitigated by the addition of a contrast matching $ZnBr_2$ solution prior to compression molding samples of TATB. Ultra small angle x-ray scattering data were acquired at the USAXS end station at the Advanced Photon Source, Argonne National Laboratory, Argonne, Illinois. Details of the technique have been described elsewhere. [16, 17].

Purity: An Agilent 1100 high performance liquid chromatography (HPLC) with diode array detector (DAD) was used for purity analysis. The mobile phase was acetonitrile: water in a 1:1 ratio. A column temperature of 40 °C with 1.2 mL/min flow rate and 10 microliters injection volume was used. Waters Atlantis T3 general purpose reverse phase C18 columns were used. TATB was dissolved in DMSO. A UV detector at 350 nm was used to detect TATB elution. Details of the procedure can be found in the new Mil spec.[18]

Powder compaction: Approximately 6 grams of TATB was added to a 1.27 cm diameter right circular die and compacted for a single cycle at 200 MPa (30 ksi) pressure in an MTS 880 hydraulic test machine under load control at a ramp rate of 26.7 N/s (6 lb/s) up and 44.5 N/s (10 lb/s) down with a 2 minute hold at maximum pressure. The actuator position was used to estimate the part density at any given time. The load during extraction was also measured under stroke control at 0.00254 cm/s (0.001 in/s). A detailed description of the experimental set up is given elsewhere [19]

One dimensional time to explosion (ODTX)

The ODTX test rapidly inserts a 1.27 cm diameter sphere of explosive into a matching spherical cavity between two heated anvils. At constant temperature the time to explosion is monitored, then the temperature is increased and a new set of anvils and explosive are tested. A detailed description of this instrument is given elsewhere [20, 21].

B. Formulation and characterization of PBX-9502

Slurry Coating, and compression molding. Lab scale, pilot scale and legacy TATB were formulated into PBX 9502-like molding powder at the 50 gram scale using a scaled down version of the Holston Slurry coating apparatus.[22, 23] This procedure was used so that as little difference as possible would be seen between legacy PBX and that made from the new TATBs. TATB and DI water were added to the coater; a solution of FK-800 in ethyl acetate was added with stirring and the solvent was driven off to

form molding powder similar to the LX-17 powder. The PBX 9502-like molding powder was dried and compression molded at various pressures into right circular cylinders ½” in diameter by 1” long at between 20-30 ksi between 100-120°C to optimize the density of the PBX.

Compressive strength . Compressive Mechanical Properties of cylinders of 9502-like PBX were measured at -20, ambient, and 50°C. A description of the method and equipment used in this test has been described elsewhere. [24]

Disc Acceleration eXperiment (DAX) performance testing of PBX-9502 formulations.

New and legacy PBX-9502 formulations were evaluated for detonation behavior using the LLNL DAX method. [25] The basic design of the DAX assembly consists of a ½-inch diameter 3 inch long sample. A combination of an RP-80 detonator and PBX-9407 booster (94% RDX, 6% FPC 461) is used to light the explosive. The detonation velocity is monitored by a series of piezoelectric timing pins mounted to a Lexan case. The relative energy and C-J pressure are calculated from the velocity of a 0.41-mm thick aluminum disc tracked using Photonic Doppler Velocimetry (PDV). An in-depth description of the method and equipment for this test is described in the reference.

Results and Discussion:

A. Neat TATB Characterization

Small Scale Safety tests. All of the new and legacy TATB drop hammer heights and BAM friction values were off scale, i.e., >177 cm and >36 kg, respectively. Spark tests also gave no reaction. All TATBs had decomposition peak temperatures in the DSC within 1 degree of each other averaging 385°C. CRT tests were higher than legacy results due to new equipment currently being used for this test. These results are shown in Table 1. Thermal analysis by DSC for several of the new DA TATB samples showed a shoulder at lower temperatures. This shoulder was increasingly evident in pilot scale TATBs (See Figures 1a, b and 2 a, b). The DSCs were run in sealed (traces in Fig 1a and 2a) and pin hole (traces in Figure 1b and 2b) pans and the pin holes seemed to enhance this shoulder at least in the ATK TATBs (compare Fig 2a and b). Although not seen in the Pantex Standard DA TATB, this shoulder has been observed in legacy dry and wet aminated TATB. [7] Currently the decomposition mechanism associated with the shoulder is not well understood but it may be associated with higher levels of fines in a given test specimen. It is known that TATB with 6 µm mean particle size has several degrees lower decomposition temperature than legacy DA TATB. [26]

Morphology, particle size distribution and crystal quality.

The morphology of new DA TATB was evaluated by SEM. Figure 3a shows SEMs of BAE (a) and ATK (b) lab scale crystals with characteristic “worm holes” of DA TATB made by the Benziger process.[27] Facets of the triclinic cell of relatively poor quality and what appear to be growth steps can readily be seen in these two micrographs. In Fig. 3b, two legacy dry aminated (C-602 and C-090), BAE (C-263) and ATK (C-627_3) pilot scale samples were compared with a legacy wet aminated TATB sample (C-084). Addition of a small percentage of water to the toluene during the amination process effectively eliminates the pock mark holes where the ammonium chloride byproduct has been removed from the DA TATB crystal

surface. The last 2 micrographs in Fig 3b and those in Figure 3c are from successive BAE pilot scale runs. As can be seen in these figures, the dry amination process can produce consistent surface morphology at the pilot scale.

Since SEM cannot reveal internal defects, polarized light micrographs were used to evaluate internal void structure of these TATB crystals. In Fig. 4a the ATK lab scale crystals were smaller and less polycrystalline than the other lab scale or standard TATB crystals. The amount of fines seems to vary with sampling. This was also observed in the light scattering measurements. In Fig 4b. crystals from the BAE (C-620 to C-622) and ATK (C-627_3-5) pilot scale runs are shown. The C-622 run was smaller than the others (similar to the ATK lab run in the previous figure). The spherical objects in some of the figures are bubbles in the high refractive index fluid used to improve the edge resolution. Two of the 3 ATK runs had low levels of fines and the C-627_4 run has very regular crystals with an aspect ratio of about 3 by comparison to the others. All of these have obvious defects distributed throughout the crystals.

Particle size distributions.

Coarse and fine peaks were observed in the scattering measurements on the Micromeritics instrument for all of the particle size distributions for the new and legacy DA TATBs. Table 2 lists the percentages of coarse and fine peaks, the mode and median with standard deviations for 3 runs of each sample. Table 2 also lists the skewness and Kurtosis on lab and pilot scale runs. The median is the 50% point of the sample of interest and the mode is the peak value in the relative frequency. A negative skewness indicates that the tail of the distribution is to the left (smaller particles) and positive skewness is the opposite. The kurtosis is related to the “thickness” of the tail or sharpness of the peak. Negative values indicate a heavier tail or more flat than a normal distribution. The median of the fine peak in all samples tested varied from 0.24-0.32 μm with small values for skew and kurtosis indicating near normal distributions. The amount of fines in a given lot varied from 7-30% with more in the BAE pilot lots, especially C-621.

In the past legacy DA TATB was manufactured by 3 different companies. The Pantex standard was from Cordova. However, legacy DA TATB from Aerojet and Rocketdyne was also available and had been evaluated on a Malvern instrument previously. Figure 5a shows data for lots from Aerojet and Rocketdyne measured on the Malvern instrument compared to the Cordova lot measured on the Micromeritics. The Micromeritics instrument seems to be much more sensitive to the fines than the Malvern, but the average values of the coarse TATB particles from the different manufactures falls between 50-70 μm .

Figure 5b shows the particle size distributions of all of the lab scale DA TATBs compared to a legacy DA TATB. The fines at the lab scale were 7-15% of the distribution, comparable or less than the standard. The average particle size of the legacy sample for ATK was 30 μm which was smaller than legacy material and BAE samples averaged about 55 μm compared to 50 μm for the Pantex standard. This is almost within the differences seen in the legacy lots. The increased prominence of fines may be associated with the Micromeritics instrument. Based on the kurtosis values the distribution of fines is

platykurtic (slightly broader than a normal distribution) and nearly symmetric but the coarse distribution is skewed toward the fines.

Figure 5c shows the particle size distributions for the BAE pilot scale runs of DA TATB. If the percentage of fines from the Micromeritics instrument measurements can be trusted, the pilot scale samples had up to twice the fines as the Pantex legacy standard, varying between 20-30% compared to about 15%, respectively. Only one run of the C-621 sample showed 30% fines, but the rest were all above 19.5%. The fines average about $\frac{1}{4}$ μm . Coarse particle size varied from 60-84 μm , close to the variation found for the 3 different manufacturer legacy samples.

The ATK pilot scale DA TATB contained 10-20% fines. So it would seem that stirring characteristics in the larger reactors are more conducive to fine production than at the laboratory scale. The coarse fraction for these TATBs varied with the PTX standard median being about 50 ± 2 μm compared to 55 ± 2 μm for the BAE lab material and 30 ± 2 μm for the ATK lab sample. The pilot scale coarse particles varied more in their median. BAE varied from 60-84 μm and between 55-72% of the distribution. ATK pilot scale coarse particles varied between 67 and 78 μm and between 75-85% of the distribution. Note that the median particle size for the ATK #4 run is smaller than the 3 and 5 runs, but the optical and SEM micrographs show larger crystals for this lot with a 3:1 aspect ratio. This appears to be due to the spherical scattering assumptions used in the light scattering computation. The percentage of coarse for ATK (C-637_4) is consistent with the optical measurements, showing the least of the ATK pilot scale TATBs.

Ultra small angle x-ray scattering

Another method used for identifying voids in a composite is small angle x-ray scattering. [16, 28] Since our main interest was the internal voids, we matched the x-ray scattering contrast of TATB with a 60% ZnBr₂/H₂O solution. This enables interrogation of internal closed porosity within the TATB. Surface scattering and regions penetrable by the solution contribute insignificantly to the scattering. In Figure 6 the USAXS results on legacy and new materials show strong similarities between the two. In the top pane, the dry powders have essentially indistinguishable scattering. This is a strong indication that, on length scales of nanometers to microns, the morphology is the same in these materials. This is in strong contrast to TATB synthesized with alternate methods that produce different morphologies and radically different x-ray scattering.[7] The lower pane in Fig. 6 shows the contrast-matched USAXS. As with the powders, the scattering is indistinguishable for a broad range of scattering angles, particularly from $q \sim 2 \times 10^{-3}$ to $q \sim 2 \times 10^{-2}$ \AA^{-1} . This area is marked 1). The scattering on these length scales is similar in all of the dry-aminated TATB lots. At lower scattering angles, there is some variation that occurs both sample-to-sample as well as, to a lesser extent, preparation-to-preparation, marked 2). There are two possibilities for this: First, incomplete filling of the intercrystalline areas could allow some empty regions to continue to scatter x-rays. Second, the hydrophobicity varies dramatically in these samples. C-623 is not presented in the lower pane because all of the preparations made with this sample showed scattering nearly identical to the dry powders, i.e., the TATB surfaces were highly hydrophobic so the solution did not wet.

Figure 7 presents derived void volume distributions from the contrast-matched USAXS, assuming three-dimensional scattering centers, i.e. the voids are more spherical than two-dimensional (disk-like) or one-dimensional (rod-like). Two peaks were observed in the distributions: One at ~100 nm, the other highly variable between ~1 and ~5 μm . As stated above, the peak marked 1) arises from fitting the scattering q -range marked in Fig.6, and is probably intracrystalline, closed porosity within TATB crystallites. Conversely, the larger variable distribution arises from the variable region in the scattering, marked with 2) in Figs. 6 (q -range) and 7 (size distribution peak). Both contrast-matched and dry powder scattering were simultaneously fit for several samples. A common distribution consistently appeared with similar sizes and volume fractions, further implying the 100 nm distribution arises from intercrystalline voids. For example, in samples C-090, C-602, and C-627, a log-normal distribution, with center parameters 132, 91, and 163 nm had volume fractions of 0.09%, 0.11%, and 0.11% respectively.

Figure 8 presents differences in scattering and derived size distributions between dry TATB powders, pressed LX-17, and contrast-matched TATB. Several interesting aspects are immediately apparent. At high scattering angles ($q > 10^{-2} \text{ \AA}^{-1}$) all approach -4 slopes in the log-log plot prior to reaching the S/N floor. This shows the smallest size regime of scatterers, and is an indication that scatterers have smooth, abrupt interfaces and are three-dimensional. The dry powders have the most intense scattering, indicating, as expected, the largest inhomogeneities in electron density, and thus greatest void volume. LX-17, as expected, gives intermediate scattering. These particular scattering curves give derived distributions in the lower pane represent about 1.1 – 1.6% of the volume for C-146 and C-063 respectively. Finally, contrast matched TATB specimens C-090 and C-627 exhibit a significant reduction in scattering in intermediate q -ranges. These have ~100 nm peaks in the void volume distributions representing .10% and .09% of the volume, respectively. These void volume distributions are plotted in the lower pane as a comparison with formulated and pressed LX-17, and give an indication of the fraction of LX-17 scatterers that are intracrystalline to the TATB, vs. additional porosity in the LX-17 existing in binder and between crystallites. The 1-5 micron peak (2) in Fig. 7 lies outside of the LX-17 sizes distribution, further evidence that the 1-5 micron peak in contrast matched arises from intercrystalline, rather than intracrystalline, porosity. This is also seen in raw, contrast-matched scattering data as the high intensity at lowest measured q -angles.

Figure 9 presents scattering acquired at larger q for these and additional samples. Although the results are qualitative, due to the setup being optimized for scattering rather than diffraction, many crystalline diffraction peaks are apparent, and all dry-aminated TATB has qualitatively identical diffraction, and thus similar molecular crystallinity. Conversely, ultra-fine TATB and TATB synthesized through other routes.[7] (C-559 and C-562) show qualitatively fewer diffraction peaks. Thus, the new dry-aminated also have more perfect crystal structures at ~nm length scales than UF or the Mantech TATBs. This may be associated with the anomalous performance of the Mantech TATBs.[7]

Purity.

LLNL was interested in getting an estimate of the purity of the Benziger DA TATB because the Mantech TATBs, TATBs recrystallized from ionic liquids and the VNS TATBs have shown anomalous results in thermal properties, density distribution[27], pbxing characteristics as well as problems in mechanical

properties and performance of PBXs made from these TATBs[29]. These issues all apparently relate to, among other things, the purity of the TATB. For example, the phloroglucinol route[4] in the Mantech effort gave only 96.56±0.01% TATB, the 3,5-Dibromoanisole route[3] gave 94.3±0.1% TATB, TATB recrystallized from ionic liquid [30, 31] was only 94.3±0.3% and the VNS TATB averaged 97.6±0.3% TATB. Table 3 shows the results of the average of 3 HPLC runs on various DA TATB samples. Without exception, these Benziger DA TATBs were very close to 100% pure, except for the Pantex legacy TATB which was 99.7%. Clearly, the material made by this method was superior to the 3 others and would not need recrystallization except perhaps for habit modification[32].

Compaction and Extraction of DA TATB powders.

Single compaction curves of density and pressure as a function of time are shown in Figure 10 for three of the 4 BAE pilot lots of DA TATB. Preliminary results (not shown) on incompletely dried powder gave anomalous results, demonstrating the importance of complete drying. For thoroughly dried powders, all of these traces look very similar. From the ratio of the part density/maximum density in the press at 30,000 psi a percentage of spring back (SB%) was estimated at between 3-3.6 %. The calculated density at maximum pressure varied between 1.82-1.90 gm/cc for a single pass and part densities varied between 1.836-1.845. Some error in the density at maximum pressure is possible due to flash being included in the part weight and the estimate of the depth of the ram in the die. Weight errors would reduce the percentage of spring back slightly. Errors in the depth of the ram in the mold would result in errors in the calculated volume at maximum pressure and therefore the density at maximum pressure and spring back values. The results are listed in Table 3. The ATK pilot scale test gave anomalous spring back results and should be retested. The densities of the parts pressed in this test were slightly higher for lab scale DA TATB compared to pilot scale. This would be consistent with more fines in the pilot scale lots compared to those made under laboratory conditions as discussed above. Pressing at 30 ksi produced viable parts without cracking, capping or major flaws.

At one of the progress reviews, Arnie Duncan, a Pantex expert in TATB characterization, mentioned that the legacy DA TATB seemed “softer” than the BAE or ATK samples. One method for estimating yield strength of powder is by calculating the aggregate yield pressure from the Heckel Equation. [33]

$$\ln[1/(1-D)] = KP + A \quad (1)$$

where D is the relative density (density at a given pressure/theoretical maximum density, TMD), P is the pressure, A and K are constants. The slope, K, has units of inverse pressure and 1/K is used as an estimate of the yield pressure, P_y for the crystal aggregates. As can be seen in Figure 11a and 11b, the low pressure end of the plots is not linear so the equation was fitted to pressures between 5000-30000 psi. When the various lab samples are plotted in this way the slope of the Pantex standard > BAE > ATK. Table 3 shows P_{y,s} of 140 < 180 < 226 MPa (20 < 26 < 33 ksi) for legacy, BAE and ATK lab scale yield pressures, consistent with Duncan’s supposition. Interestingly the BAE pilot scale yield pressures are closer to and in one case less than the legacy Pantex standard. However the ATK pilot lot that was tested was “hard” like the ATK lab scale DA TATB. These differences appear to be associated with the strength of the aggregates that form during the precipitation of the DA TATB in the amination step and possibly

by the particle size distribution. The Heckel equation intercept is related to the relative density where the particle begins to deform inelastically, D_a . For the DA TATBs this value runs around 78-79% of TMD.

The extraction force as the compacted part is being removed from the die was also monitored. If the radial pressure between the die and the part is uniform after compaction, once the initial separation from the wall is accomplished, the part should move along the die at a constant force due to friction between the TATB and the die wall. As can be seen in Figure 12a and 12b, initially the force increases rapidly but once the part starts to move, the force becomes nearly constant until the part exits the die. When the part begins to exit the die, the force decreased linearly because wall friction is no longer affecting the portion of the sample that had already exited the die. The Pilot scale DA TATBs from ATK and BAE were similar to or required slightly lower force for the part to be extracted from the die. At a value of -1.5 inches of stroke motion, the part falls out of the die and the load becomes zero. Extraction pressures around 7-10 MPa (1000-1500 psi) are quite low probably because of the graphitic nature of TATB produced by the Benziger process.

One dimensional time to explosion (ODTX):

One of the BAE pilot scale DA TATB samples (C-620) was molded into spheres and compared to data from ultrafine, wet aminated and a legacy material of unknown origin. As can be seen in Figure 13, the new BAE material is comparable to the other legacy TATBs with similar particle size whereas the ultrafine TATB is slightly less thermally stable.

B. Formulation and Properties of PBX-9502 made from legacy and new DA TATBs

Slurry coating: The Holston proprietary procedure for formulating PBX 9502 was scaled down to 50 grams except that more water was required to cover the impeller and baffles completely. Beads were about the same size as legacy PBX 9502 molding powder, but with larger amounts of fines. Figure 14 shows the steps in the process. Typically the aqueous slurry of TATB is agitated while the binder lacquer is added slowly. Almost immediately upon addition of the lacquer, the binder in the lacquer begins to precipitate on the TATB in the slurry and molding powder beads are formed. In the case of PBX 9502 and LX-17-0 the binder is Kel-F 800 at 5 and 7.5%, respectively. As the solvent is driven off by heating, the beads harden and can be filtered in a large Buchner funnel to dewater. After drying to remove any residual water or solvent, the dry molding powder can be compression molded or isostatically pressed and machined to almost any desired shape.

Density: The density of molded parts is critical because it controls the properties of interest for the plastic bonded explosive. The density of compression molded parts from legacy PBX-9502, and samples from the slurry coater are compared in Table 4. Densities of the pilot and Pantex legacy TATBs formulated into PBX-9502 using the 50 gram BAE procedure and compression molded into 1 x 0.5" cylinders with a 3 cycle 30 ksi pressing routine at 120°C gave densities within 1.893 ± 0.002 gm/cc. These results compare well with PBX 9502 formulated at HAAP (1.891 ± 0.013 gm/cc). This is only about 95.8% of the theoretical maximum density, but PBX 9502 is known to be starved for binder.

Mechanical Properties: It has been shown that remarkably consistent modulus (std dev ~1%) , peak stress (std. dev. ~0.3%) and strain(std. dev. ~0.7%) are obtained when a production lot of PBX-9502 is isostatically pressed and thermally conditioned in a consistent way.[34] When legacy PBX-9502 from different lots is compared more scatter is observed, often several percent differences in strength (peak stress) and 10% or more in modulus. However, previous comparisons of legacy LX-17 with LX-17-like formulations based on MANTEC TATB were dramatically different showing 2 times more strength and modulus for formulations based on very small particle size.[29] Similar increases in modulus and strength but reduction in strain was observed when recycled TATB was used to make PBX-9502.[35] In Figure 15a Pantex legacy TATB (C-602) formulated into PBX-9502 at the 50 gram level and compression molded is compared to PBX-9502 machined from isostatically pressed parts at 3 temperatures (-20, 23 and 50°C). The isostatically pressed PBX 9502 had higher modulus at all three temperatures than the 50 gram PBX made from the Pantex standard but lower elongation except cold and lower or comparable strength. Some of this is probably due to crystal development in the binder, but this should be least observable cold. Clearly there are differences between the 50 gm batch of 9502-like PBX made from legacy C-602 TATB and legacy PBX-9502 made by isostatic pressing and machining.

The compressive mechanical properties of the PBX-9502-like formulation made from BAE C-621 pilot scale DA TATB are compared to legacy PBX-9502 described above in Figure 15b. Again, the moduli of the 50 gram slurry coated formulation which was compression molded are lower than the historical tests, but much closer than the PTX standard formulation. Here again, lower modulus and higher elongation at 50°C, is indicative of lower crystallinity in the FK-800 binder. Since the glass transition of FK-800 is about 25°C, the effect of binder crystallinity should be virtually eliminated at ambient and -20°C. However, the modulus was always lower for the small formulations. In this case the elongation and strength were fairly similar. In the BAE case, two formulations were made from the same pilot scale lot. As can be seen in the figure, the reproducibility of the small 50 gm. mixes is excellent. This would seem to imply that things like particle size distribution, aging and post formulation processing play a significant role in the mechanical behavior.

Figure 15c is a plot of compressive properties of the C-627-3 BAE DA TATB formulated into 9502-like PBX compared to legacy PBX-9502. The ATK formulation is fairly similar to the legacy DA TATB formulation and not as close to PBX-9502 as the BAE formulation. Here again the elongation at elevated temperature is higher while the modulus and strength are reduced compared to legacy PBX-9502 described above. This is consistent with the lack of binder crystallinity in newly pressed parts. Why this carries over into the lower temperatures is as yet unclear. Table 5 lists the values for Young's modulus (E_y), maximum stress (σ_{max}), strain at maximum stress (ϵ_{max}), and stress and strain at break (σ_b) and (ϵ_b), respectively for all of the compression tests.

Performance: The performance of the PBX-9502-like formulations was evaluated using the LLNL DAX test. Figure 16 shows a schematic of the test and the velocity of the aluminum flyer for 5 different tests. The Chapman-Jouguet (CJ) pressure is estimated from an extrapolation of the plate jump-off velocity to zero and then using impedance matching techniques. [36] As seen in the figure, there is considerable noise in the first valley behind the first spike in these traces possibly associated with after burn chemistry. This can cause some variability in the CJ pressure (P_{c_j}) estimate. Even so P_{c_j} averages about

27.1 ± 0.6 GPa with Legacy PBX 9502 being the highest (see Table 6). The detonation velocity averaged about 7.47 ± 0.03 mm/μs and with one of the BAE 9502-like formulations being the fastest, but none being beyond one standard deviation. Finally at moderate expansion the square of the aluminum flyer velocity is proportional to the energy of the explosive. When the limiting flyer velocity is used to estimate the energy, as can be seen in the table and figure, the same BAE sample was about 4% higher in energy than the legacy PBX 9502. Within the assumptions associated with this energy calculation, these samples produce approximately the same energy.

Conclusions:

There are interesting differences between the legacy TATB and the two new Benziger TATBs from BAE and HAAP. Although, as expected, the classic small scale safety tests are off scale for this “wooden” explosive and the morphologies are characteristic of DA TATB, particle sizes varies in a similar manner to what has been seen in lots from the 3 different legacy DA TATB producers. Both DSC and ODTX indicate no reduction of thermal stability in either of the new DA TATBs. Evidence of increased fines in the pilot scale runs may be a statistical anomaly or an instrument issue, but deserves a revisit for the DA TATB production material. Crystal quality is not the greatest based on USAXS data, but, of course, reduced sensitivity TATB seems to be an oxymoron. If the differences in compaction of TATB (harder TATB) are associated with aggregate strength, this may go away at the production scale.

The 9502-like formulations made from legacy and new DA TATB, could be formulated into molding powder in the small scale slurry coater which was similar to legacy production PBX 9502 molding powder and excellent densities were obtained from compression molding at appropriate temperature, pressure and cycles, but differences in mechanical properties were observed. Because of the similarity between the new BAE TATB and legacy PBX-9502 mechanical properties, the differences between small versus larger scale slurry coating of DA TATB do not appear significant. This being the case, why were the legacy DA TATB and ATK DA TATB so similar, but different from the legacy PBX 9502 and 9502-like BAE formulation? Despite these mechanical dissimilarities, parts could be made at reasonable densities from all the small scale formulations and the performance, as estimated from the DAX tests, compared very well to legacy PBX-9502.

Although there were slight differences in these tests, the general conclusion was that the new DA TATBs were sufficiently similar to legacy material to be suitable replacements for any DOE requirements for DA TATB. This does not remove the necessity of evaluating explosives formulated from this material in future systems, but does show high probability of success using the new DA TATBs as a replacement for legacy DA TATB in PBXs and weapons systems without compromising performance or safety.

Acknowledgements:

Those of us at LLNL are grateful to the DoD and DOE for the opportunity to be part of the team that resurrected this process for synthesizing TATB in production quantities. Special thanks go to Crane Robinson from Picatinney Arsenal who lead the program and Tim Mahoney as the chief scientist involved in the effort. We also wish to acknowledge Lew Steinhof who took the project under his wing on the DOE side. Numerous people provided the data used in this report. Fowzia Zaka made psd measurements and took the SEM micrographs. Heidi Turner and Jenifer Montgomery ran the DSC

measurements. The other small scale safety data were generated by Pete Nunes and Gary Hust. The ODTX data was provided by Peter Hsu. We also acknowledge many useful discussions with the DOD-DOE TATB working group and members of the teams from ATK and BAE who did the real work.

References:

1. Benziger, T.M., "Manufacture of Triaminotrinitrobenzene," in *Chemical and Mechanical Technologies of Propellants and Explosives, Proc. 1981 Intl. Annual ICT Conference* 1981: Karlsruhe, Germany.
2. Calvert, P., *Inkjet Printing for Materials and Devices*. Chem. Mater., 2001. **13**: p. 3299-3305.
3. Sleadd, B., *Synthesis and Scale-up of sym-triaminotrinitrobenzene at Holston Army Ammunition Plant*, in *IM&EM Technology Symposium* 2006, NDIA: Bristol, UK.
4. Velarde, S., *Pilot Plant Synthesis of Triaminotrinitrobenzene (TATB)*, in *2006 IM/EM Technical Symposium* 2006, April 24-28, NDIA: Bristol, UK.
5. Bellamy, A.J., S.J. Ward, and P. Golding, *A new synthetic route to 1,3,5-triamino-2,4,6-trinitrobenzene (TATB)*. Propellants Explosives Pyrotechnics, 2002. **27**(2): p. 49-58.
6. Hoffman, D.M., T.M. Willey, and S.C. DePiero, *A Comparison of New TATBs, FK-800 binder and LX-17-like PBXs to Legacy Materials*, in *1st Korean International Symposium on High Energy Materials* 2009, LLNL-CONF-412929, Lawrence Livermore National Laboratory: Incheon, South Korea.
7. Hoffman, D.M., et al., *Comparison of New and Legacy TATBs*. Journal of Energetic Materials, 2008. **26**(3): p. 139-162.
8. Clements, B., et al., *KEL-F 800 EXPERIMENTAL CHARACTERIZATION AND MODEL DEVELOPMENT*, 2007, Los Alamos National Security. p. 1-192.
9. Simpson, R.L., Foltz, M.F., *LLNL Small-Scale Drop-Hammer Impact Sensitivity Test*, 1996, UCRL-ID-119665, Lawrence Livermore National Laboratory, Livermore, CA 94550.
10. Simpson, R.L., Foltz, M.F., *LLNL Small-Scale Friction Sensitivity (BAM) Test*", 1996, UCRL-ID-124563, Lawrence Livermore National Laboratory, Livermore, CA 94550.
11. Simpson, R.L., Foltz, M.F., "LLNL Small-scale Static Spark Machine: Static Spark Sensitivity Test", 1995, UCRL-ID-135525, Lawrence Livermore Laboratory, Livermore, CA.
12. Mellor, A.M., Covino, J., Dickenson, C.W., Dreitzler, D., Thorn, L. B., Frey, R. B., Gibson, P.W., Roe, W. E., Kirshenbaum, M. and Mann, D. M., *Hazard Initiation in Solid Rocket and Gun Propellants and Explosives*. Prog. Energy Combust. Sci., 1988. **14**(213).
13. RISI, *Technical Discussion On Explosives and EBW detonators*, I. Reynolds Industries, Editor 2000.
14. Gash, A.E., et al., *Environmentally Benign Impact Initiated Devices Using Energetic Sol-Gel Coated Flash Metal Multilayers*, 2003: LLNL.
15. Alexander Gash, et al., *Environmentally Benign Stab Detonators PP-1362*, 2003, Lawrence Livermore National Laboratory: Livermore, CA.
16. Willey, T.M., et al., *The Microstructure of TATB-Based Explosive Formulations During Temperature Cycling Using Ultra-Small-Angle X-Ray Scattering*. Propellants Explosives Pyrotechnics, 2009. **34**(5): p. 406-414.
17. Willey, T.M., et al., *In-Situ Monitoring of the Microstructure of TATB-based Explosive Formulations During Temperature Cycling Using Ultra-small Angle X-ray Scattering*. Propellants Explosives Pyrotechnics, 2008. **in press**.
18. Defense, D.o., *Draft MIL-DTL-32337 (OS) Triaminotrinitrobenzene (TATB)* 2013, Department of Defense: Washington, DC. p. 1-40.

19. M. Gresshoff and D.M. Hoffman, *LLNL-CONF-514891 - Compression Molding of UFTATB with Various Mold Releases*, in *2012 Insensitive Munitions and Energetic Materials Technology Symposium*, 2012, NDIA: Las Vegas, NV, USA.
20. Hsu, P.C., *LLNL-BR-411732, "LLNL ODTX System for Thermal Safety Determination of Energetic Materials"*, 2009, Lawrence Livermore Laboratory: Livermore, CA 94550. p. 1-9.
21. Hsu, P.C., M. Howard, and G. Hust, *One-Dimensional Times to Explosion (Thermal Sensitivity) and Small-scale Safety Testing of TMI TATB Formulations*, 2009, Lawrence Livermore Laboratory: Livermore, CA 94550. p. 1-9.
22. DePiero, S.C. and D.M. Hoffman, *Formulation and Characterization of LX-17-2 from new FK 800 binder and WA, ATK, and BAE TATBs*, 2007, LLNL-TR-416360, Lawrence Livermore National Laboratory, Livermore, CA 94550. p. 1-18.
23. Kasprzyk, D.J., et al., *Characterization of a slurry process used to make a plastic-bonded explosive*. *Propellants Explosives Pyrotechnics*, 1999. **24**(6): p. 333-338.
24. Groves, S., et al., *Tensile and Compressive Properties of Billet Pressed LX17-1 as a Function of Temperature and Strain Rate*, 2000, Lawrence Livermore National Laboratory.
25. Lorenz, K.T. and E.L. Lee, *DAX: A TOOL FOR RELIABLE, SMALL-SCALE PERFORMANCE CHARACTERIZATION OF ENERGETIC MATERIALS*, 2012, Lawrence Livermore National Laboratory: Livermore, CA. p. 1-10.
26. Koerner, J., et al., *ODTX Measurements and Simulations on Ultra Fine TATB and PBX-9502*, in *North American Thermal Analysis Society 35th Annual Conference 2007*, NATAS: East Lansing, MI.
27. Hoffman, D.M. and A.T. Fontes, *Density Distributions in TATB Prepared by Various Methods*. *Propellants Explosives Pyrotechnics*, 2010. **35**: p. 15-23.
28. Willey, T.M., et al., *Changes in pore size distribution upon thermal cycling of TATB-based explosives measured by ultra-small angle X-ray scattering*. *Propellants Explosives Pyrotechnics*, 2006. **31**(6): p. 466-471.
29. DePiero, S.C. and D.M. Hoffman, *Formulation and Characterization of LX-17-2 from new FK 800 binder and WA, ATK, and BAE TATBs*, 2007, Lawrence Livermore National Laboratory, Livermore, CA 94550.
30. Han, T.Y.J., et al., *The solubility and recrystallization of 1,3,5-triamino-2,4,6-trinitrobenzene in a 3-ethyl-1-methylimidazolium acetate-DMSO co- solvent system*. *New Journal of Chemistry*, 2009. **33**(1): p. 50-56.
31. Zhu, H.X., et al., *An environmental friendly approach for the synthesis of the ionic liquid 1-ethyl-3-methylimidazolium acetate and its dissolubility to 1, 3, 5-triamino-2, 4, 6-trinitrobenzene*. *Journal of Molecular Liquids*, 2012. **165**: p. 173-176.
32. Zhang, H.B., et al., *Crystal Morphology Controlling of TATB by High Temperature Anti-Solvent Recrystallization*. *Propellants Explosives Pyrotechnics*, 2012. **37**(2): p. 172-178.
33. Heckel, W., *An analysis of powder compaction phenomena*. *Trans. Metall. Soc AIME* 1961. **221**: p. 671-675.
34. Gagliardi, F., B. Cunningham, and S. Pease, *Binder Aging Studies on PBX-9502*, 2013, Lawrence Livermore National Laboratory: Livermore, CA. p. 1-25.
35. Peterson, P.D. and D.J. Idar, *Microstructural differences between virgin and recycled lots of PBX 9502*. *Propellants Explosives Pyrotechnics*, 2005. **30**(2): p. 88-94.
36. Kury, J.W., et al., *Metal Acceleration by Chemical Explosives*, in *Proceedings Fourth Symposium (International) on Detonation* 1965, Department of the Navy: White Oak, MD. p. 3-13.

Table 1. LLNL Small scale safety test results were very similar for lab and pilot scale TATB compared to legacy dry aminated TATB. Lots shown are LLNL lot numbers.

SSS test	LLNL Lot #	DH 50	BAM	Spark	CRT cc./25g	DSC Ton	Tpeak (°C)	ΔH_d (kJ/gm)
Legacy	C-090	>177 cm	>36 kg	NS	0.004±2	344	378±0.3	1.1±0.5
ATK L	C-601	>177cm	>36 kg	NS	0.013±5	350	385.2±.2	1.3±2
BAE L1	C-605	>177cm	>36 kg	NS	0.014	350	384.2±0.3	2.0±7
BAE L6	C-606	>177cm	>36 kg	NS	0.02	348	383.8±0.4	1.7±5
BAE L3	C-607	>177cm	>36 kg	NS	0.052	350	384.6±0.4	1.6±3
PTX DA	C-602	>177cm	>36 kg	NS	0.028	350	384±1	1.5±3
BAE P6	C-620	>177cm	>36 kg	NS	0.056	350	384.6	1.3
BAE P4	C-621	>177cm	>36 kg	NS	0.062	350	384	2.0
BAE P5	C-622	>177cm	>36 kg	NS	0.006	350	384	1.7
BAE P7	C-623	>177cm	>36 kg	NS	0.030	348	385	1.6
ATK P3	C-627_3	>177cm	>36 kg	NS	0.046	350	383.2	2.0
ATK P4	C-627_4	>177cm	>36 kg	NS		348	384.2	1.5
ATK P5	C-627_5	>177cm	>36 kg	NS		350	384.1	1.5

Table 2. Comparable particle size distributions for TATBs with legacy TATBs were found.

Peak #	% Dist.*	Mode	Std Dev	Median	Std Dev	Skewness	Kurtosis
B-684 (LLNL)	98.4	52.1	0.0	48.2	1.0	-1.25	0.154
B-685 (LLNL)	97.2	52.1	0.0	47.1	0.2	-1.36	0.477
C-090 (LLNL)	99.4	82.4	0.0	72.4	2.2	-1.16	0.002
C-602(PTX)							
Peak 1	13.5	0.299	0.024	0.237	1.649	-0.039	-0.705
Peak 2	83.8	69.45	4.70	49.11	2.256	-0.968	0.335
Peak 1 (2)	13.5	0.25	0	0.247	1.686	-0.013	-0.697
Peak 2 (2)	83.9	69.68	8.547	48.92	2.284	-0.983	0.347
C-601(ATK)							
Peak 1	10.4	0.282	0.0	0.265	1.733	-0.023	-0.737
Peak 2	87.2	31.6	0.0	29.8	1.87	-0.475	0.255
Peak 1 (2)	10.2	0.245	0.002	0.265	1.733	-0.030	-0.722
Peak 2 (2)	87.7	31.6	1.02	29.68	1.847	-0.480	0.148
C-605(BAE)							
Peak 1 (2)	14.8	0.256	0.023	0.257	1.716	-0.024	-0.730
Peak 2 (2)	78.9	63.0	0.0	54.56	1.906	-0.462	-0.320
Peak 1	12.0	0.273	0.011	0.245	1.665	-0.073	-0.747
Peak 2	83.8	63.0	0.0	55.20	2.015	-0.475	-0.135

C-606(BAE)							
Peak 1	7.6	0.316	0.026	0.304	1.885	0.056	-0.702
Peak 2	90.5	66.73	0.0	55.71	2.045	-0.530	-0.236
Peak 1 (2)	6.6	0.318	0.041	0.322	1.864	-0.064	-0.755
Peak 2 (2)	91.2	70.68	0.0	55.54	2.021	-0.510	-0.260
C-607(BAE)							
Peak 1	9.0	0329	0.028	0.310	1.901	0.054	-0.718
Peak 2	89.0	66.73	0.000	56.61	1.913	-0.574	-0.089
C-620 (BAE)							
Peak 1	20.8	0.265	0.0	0.248	1.692	-0.016	-0.708
Peak 2	72.6	74.9	2.964	60.24	2.164	-1.016	0.325
Peak 1 (2)	24.6	0.250	0.0	0.233	1.636	-0.044	-0.708
Peak 2 (2)	70.2	74.9	0.0	60.37	2.167	-1.142	0.724
C-621 (BAE)							
Peak 1	29.9	0.25	0.0	0.234	1.639	-0.041	-0.703
Peak 2	54.8	90.0	0.0	84.36	1.403	-0.477	-0.052
Peak 1 (2)	22.3	0.25	0.0	0.236	1.645	-0.047	-0.709
Peak 2 (2)	61.1	88.9	0.0	84.50	1.379	-0.475	-0.169
C-622							
Peak 1	20.35	0.265	0.0	0.242	1.6645	-0.0415	-0.717
Peak 2	66.6	74.85	0.0	75.995	1.464	-0.801	0.434
Peak 1 (1)	19.5	0.255	0.008	0.244	1.671	-0.037	-0.718
Peak 2 (1)	67.1	84.0	0.0	76.19	1.445	-0.777	0.356
C-623							
Peak 1	20.9	0.251	0.0	0.238	1.653	-0.035	-0.697
Peak 2	67.3	84.01	0.0	79.93	1.486	-0.920	0.728
Peak 1 (1)	19.4	0.255	0.008	0.237	1.648	-0.039	-0.701
Peak 2 (1)	72.0	84.01	0.0	78.59	1.637	-1.139	1.157
C-627_3 ATK							
Peak 1	13.5	0.281	0.0	0.260	1.720	-0.028	-0.724
Peak 2	80.4	80.9	2.7	74.95	1.593	-1.081	1.202
Peak 1 (2)	19.7	0.271	0.009	0.247	1.682	-0.030	-0.703
Peak 2 (2)	73.7	79.3	0.0	74.76	1.578	-1.059	1.194
C-627_4 ATK							
Peak 1	11.5	0.336	0.038	0.309	1.851	-0.025	-0.746
Peak 2	84.8	64.2	2.2	67.25	1.403	-0.582	0.554
Peak 1 (2)	11.3	0.325	0.06	0.298	1.792	-0.080	-0.760
Peak 2 (2)	84.8	64.20	2.2	66.75	1.410	-0.589	0.629
C-627_5 (ATK)							
Peak 1	16.6	0.261	0.009	0.245	1.674	-0.031	-0.704
Peak 2	76.1	84.0	0.0	78.65	1.497	-1.101	1.649
Peak 1 (2)	18.3	0.265	0.015	0.247	1.681	-0.029	-0.709
Peak 2 (2)	74.6	84.0	0.0	78.68	1.515	-1.253	2.188

* Peaks at least 5.00 % of the Distribution

Table 3. Purity and Powder compaction results for new and legacy dry aminated TATBs produced part densities for a single pass of about 95% TMD.

Sample	lot	Purity	$\rho(\text{max})$	$\rho(\text{part})$	SB (%)	$K \cdot 10^{-5}$	a	Py (MPa)
Ptx Std	C-602	99.73±0.06	1.8875	1.8453	3.22	7.16	1.35	96.2
ATK L	C-601	102.95±0.01	1.8286	1.8436	3.22	4.43	1.52	156
BAE L	C-607	100±0.04	1.8618	1.8435	3.33	5.56	1.52	124
BAE P	C-620	101±2						
BAE P	C-621	100±2	1.8915	1.8362	2.92	6.77	1.54	102
BAE P	C-622	100.5±0.5	1.9056	1.8358	3.66	4.74	1.56	146
BAE P	C-623	98±2	1.8945	1.8356	3.11	4.61	1.53	149
ATK#3	C-627_3		1.7602	1.8397	-4.4	2.97	1.52	232

Table 4. Compression molding densities of PBX-9502 legacy material compared to ATK, BAE and Pantex Standard TATBs formulated into PBX-9502-like explosives at the 50 gram level.

	BAE C-620 #1	BAE C-620 #2	PTX Std (C-602) #1	ATK C627_3 #1	*PBX9502 C-382
Part #	ρ (gm/cc)	ρ (gm/cc)	ρ (gm/cc)	ρ (gm/cc)	ρ (gm/cc)
#1	1.8952	1.8920	1.8928	1.8980	1.876
#2	1.8940	1.8950	1.8930	1.8981	1.894
#3	1.8938	1.8957	1.8951	1.8959	1.895
#4	1.8933	1.8957	1.8945	1.8869†	1.897†
#5	1.8894	1.8944	1.8948	1.8886†	1.897†
#6	1.8903	1.8966	1.8967	1.8877†	1.898†
#7	1.8939	1.8936		1.8902†	1.863†
Avg.	1.893±0.001	1.895 ± 0.002	1.895±0.002	1.892±0.004	1.891±0.013

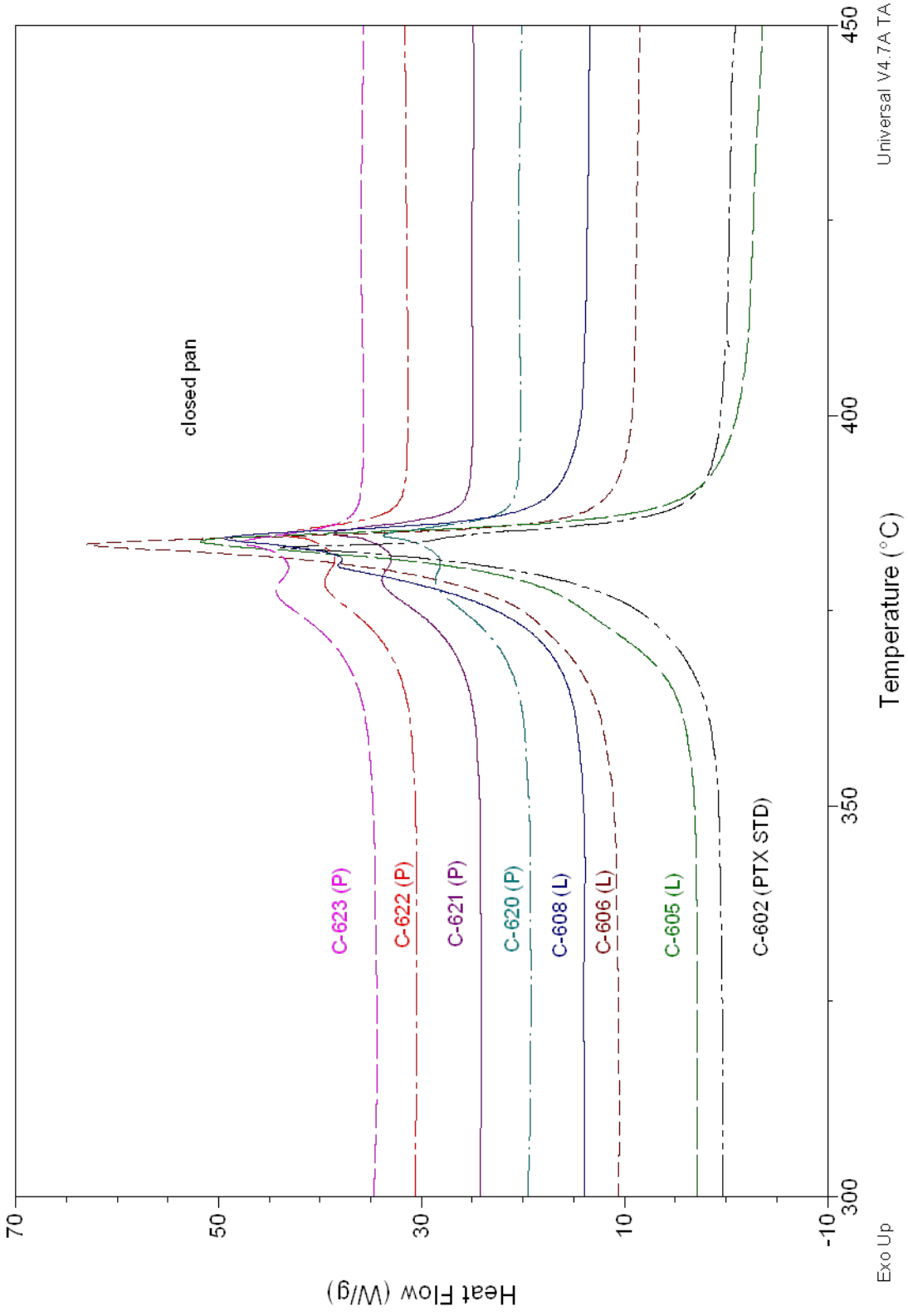
*T=110°C; † half inch long parts rather than 1”.

Table 5. Mechanical properties of various PBX-9502-like TATB slurry coated formulations were compared to legacy PBX-9502.

TATB	Lot #	C-620	C-620	Legacy	627_3	C-602
Temperature	Prop	BAE1	BAE2	9502	ATK	PTX
-20°C	E_y	8.98E+05	8.19E+09	1.10E+06	7.43E+05	4.47E+05
	R	0.99885	0.9996	0.99984	0.99928	0.9978
	σ_{max}	4930.5	4954.7	4795.2	4396.4	5379.3
	ϵ_{max}	2.31%	2.50%	2.11%	2.13%	2.94%
	σ_b	4900	4800	4500	--	5230
	ϵ_b	2.80%	3.50%	4.22	--	3.39%
23	E_y	6.39E+05	7.38E+05	7.84E+05	7.09E+05	3.68E+05
	R	0.99785	0.99934	0.99953	0.99941	0.99744
	σ_{max}	3109	3067	3188.6	2603.3	3399.3
	ϵ_{max}	2.67%	2.30%	2.27%	18.80%	3.05%
	σ_b	2750	2700	2910	2400	3000
	ϵ_b	5%	4.05%	4.13%	3.39%	4.98%
50	E_y	3.80E+05	3.42E+05	5.42E+05	4.44E+05	1.81E+05
	R	0.9972	0.9956	0.99882	0.99631	0.9949
	σ_{max}	1751.8	1741.3	1942.1	1553	1795.8
	ϵ_{max}	2.24%	2.43%	1.81%	2.19%	2.88%
	σ_b	1380	1500	1800	1270	1640
	ϵ_b	4.34%	4.06%	2.80%	4.10%	3.60%

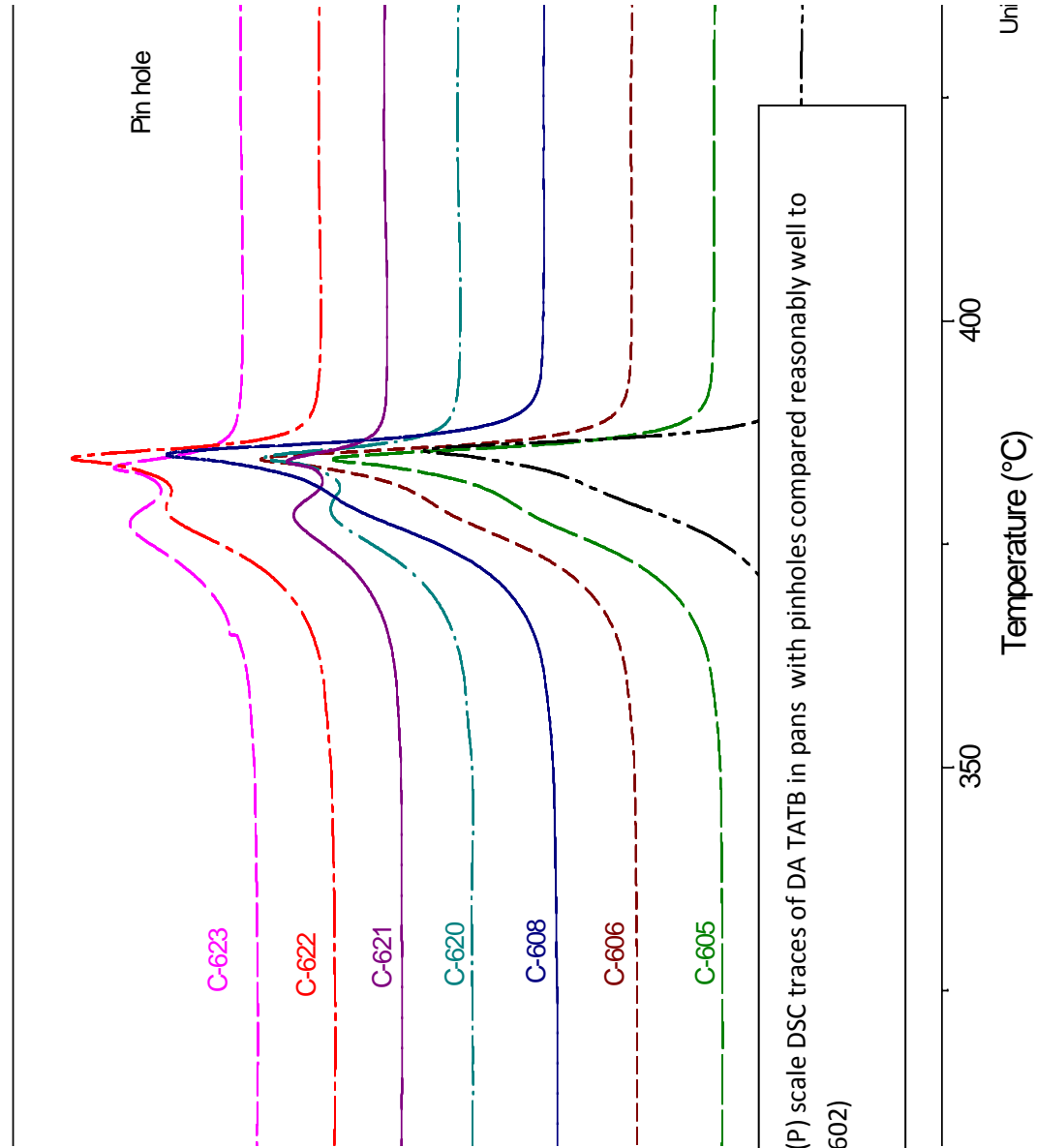
Table 6. Detonation velocities, Chapman-Jouguet (CJ) pressures, and relative energies for and PBX-5902-like formulations with new and legacy DA TATB compared well with legacy PBX 9502.

Batch	Density (g/cc)	Detonation Velocity (m/s)	CJ Pressure (GPa)	Metal Velocity (m/s)	Relative Metal Energy
PBX-9502	1.887	7.480	27.8	4471	1
(Adapt)					
PX DA-TATB	1.894	7.500	27.4	4445	-1.2%
BAE #2 (Shot 7)	1.891	7.430	27.0	4431	-1.8%
BAE #2 (Shot 8)	1.894	7.490	26.3	4557	+3.9%
ATK #6	1.897	7.431	27.2	4435	-1.6%
uf-TATB	1.800	7.416	26.6	4568	+4.4%



Universal V4.7A TA Instruments

Figure 1a. BAE lab (L) and pilot (P) scale DSC traces of DA TATB in hermetically sealed pans compared reasonably well to legacy DA TATB from Pantex (C-602)



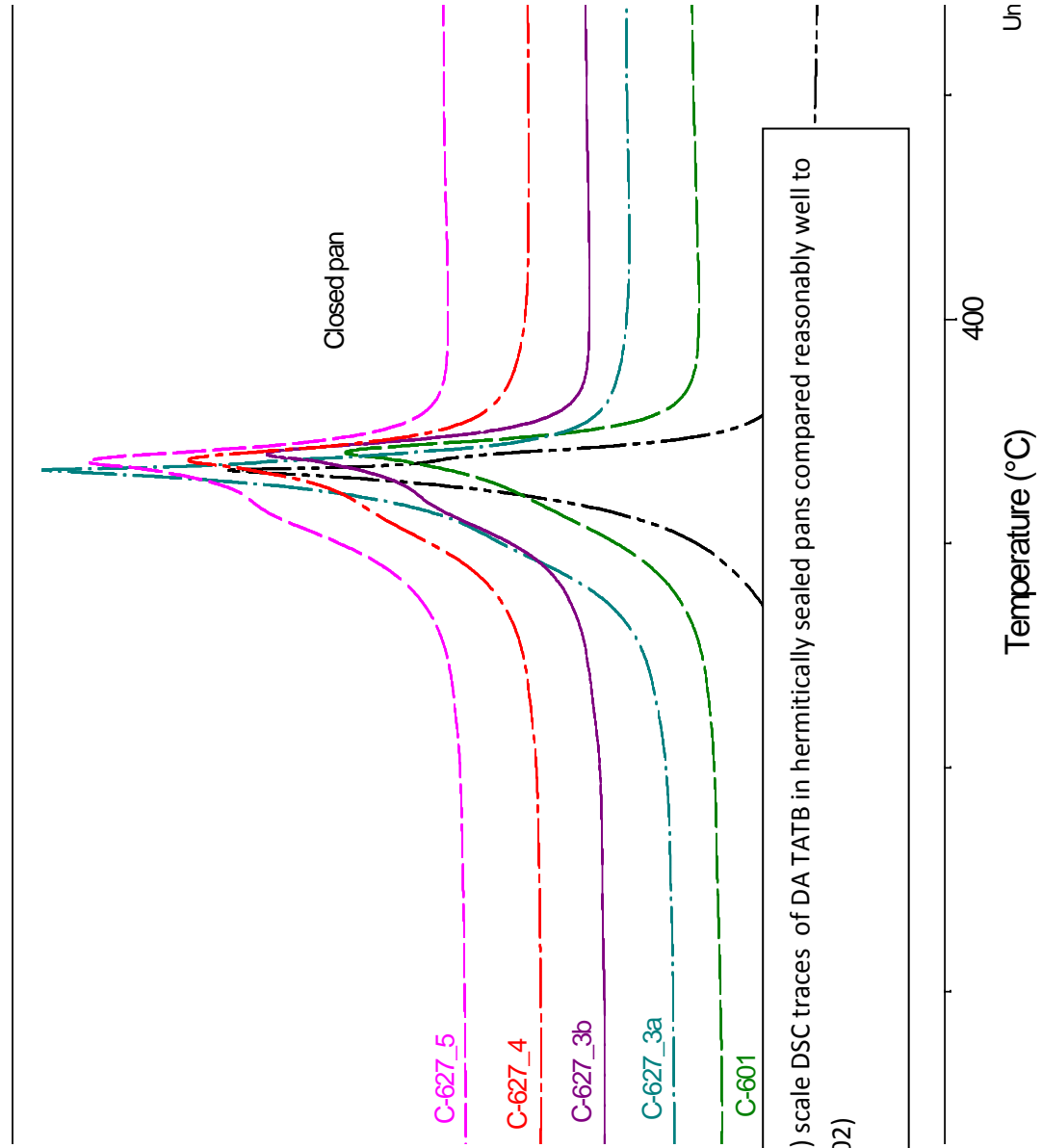
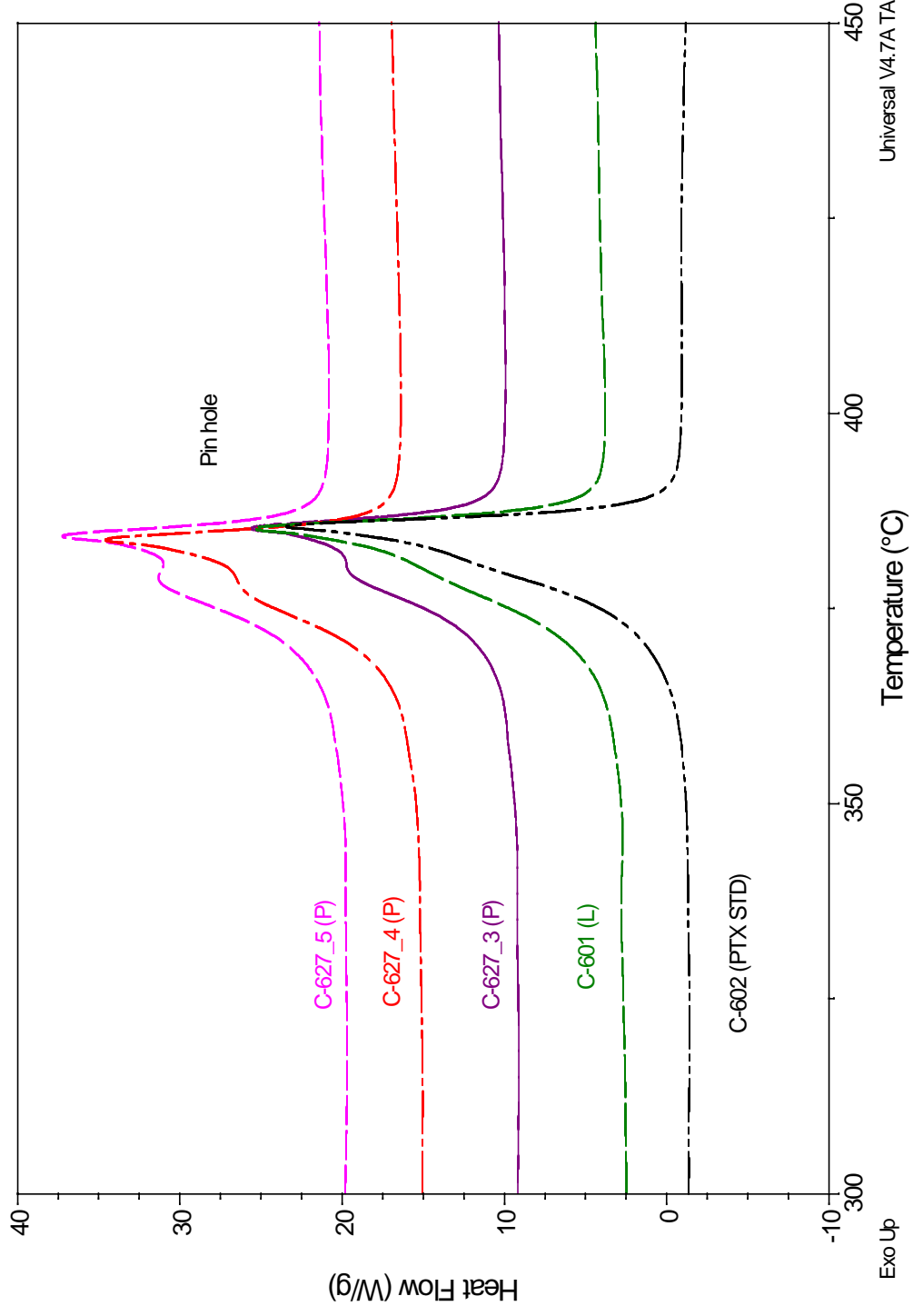


Figure 2a. ATK lab (L) and pilot (P) scale DSC traces of DA TATB in hermitically sealed pans compared reasonably well to legacy DA TATB from Pantex (C-602)



Universal V4.7A TA Instruments

Figure
legacy

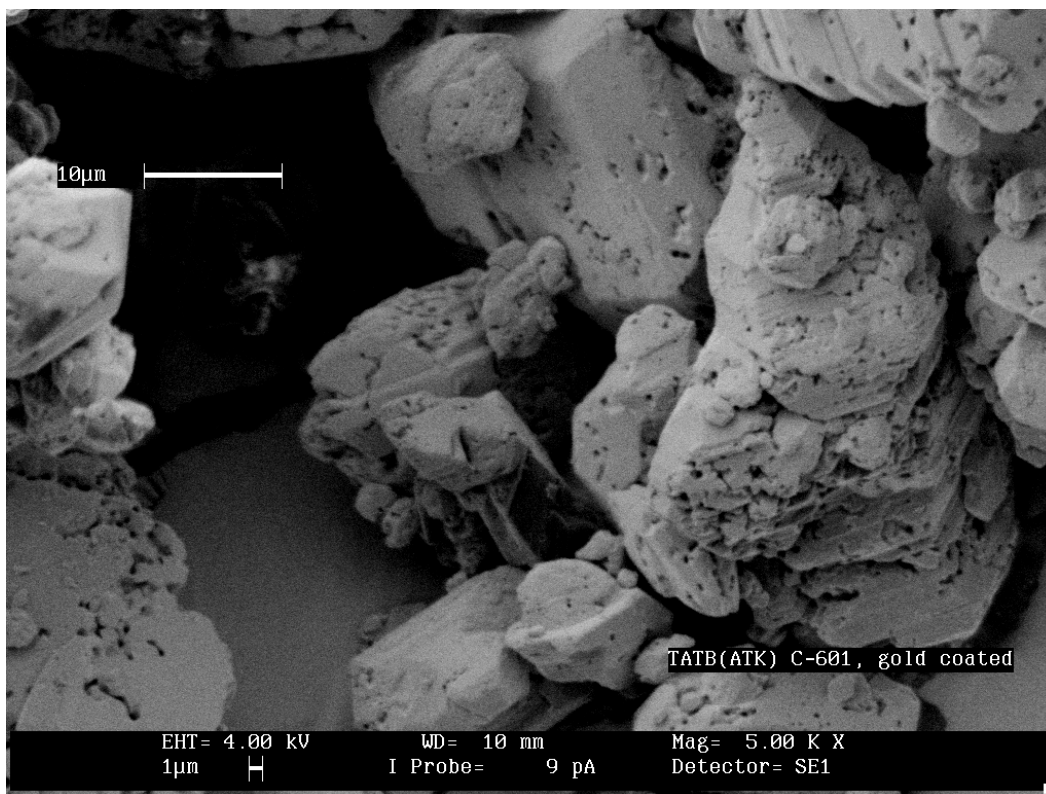
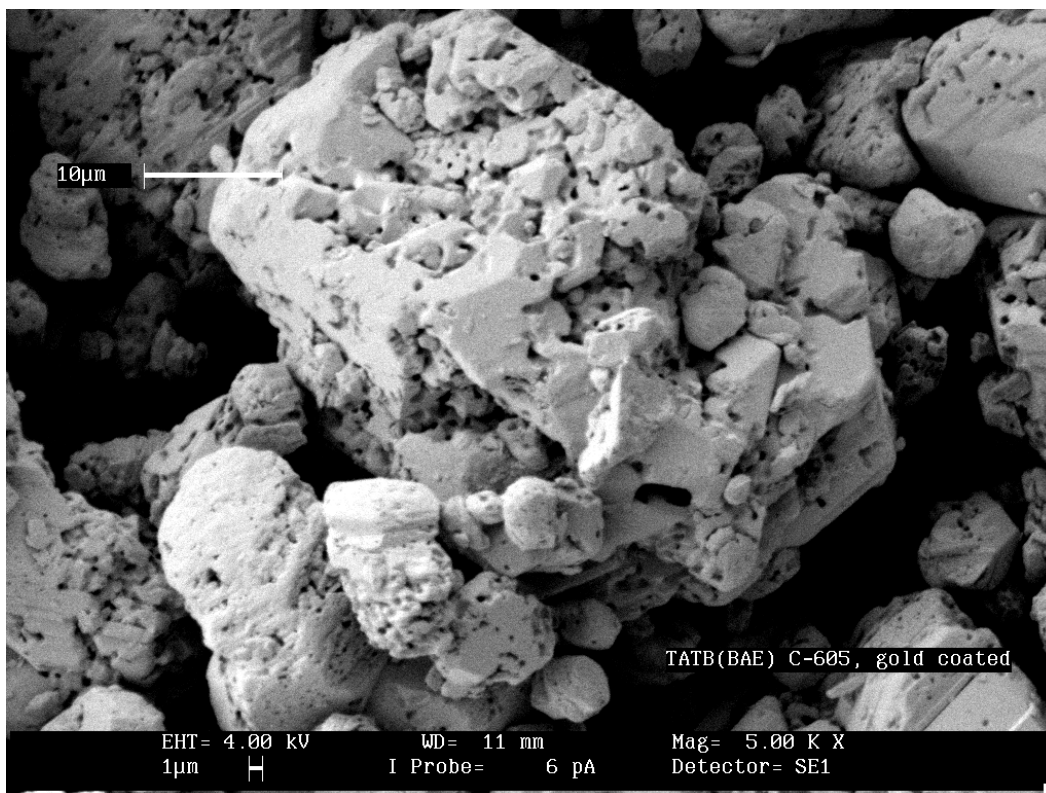


Figure 3a. SEMs of lab scale TATB from ATK and BAE contained “worm holes” characteristic of legacy dry aminated TATB.

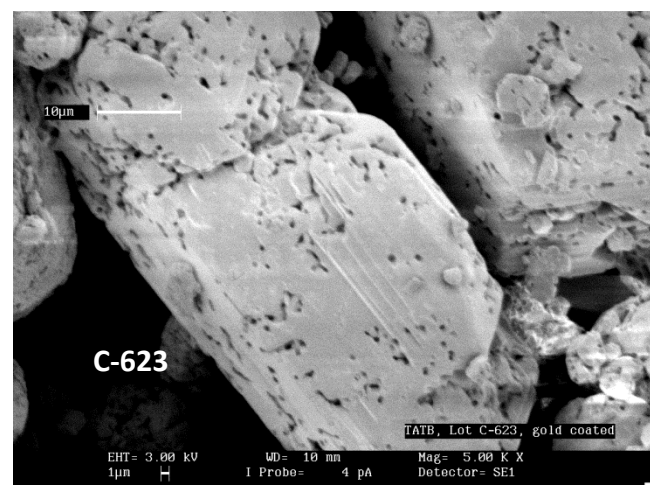
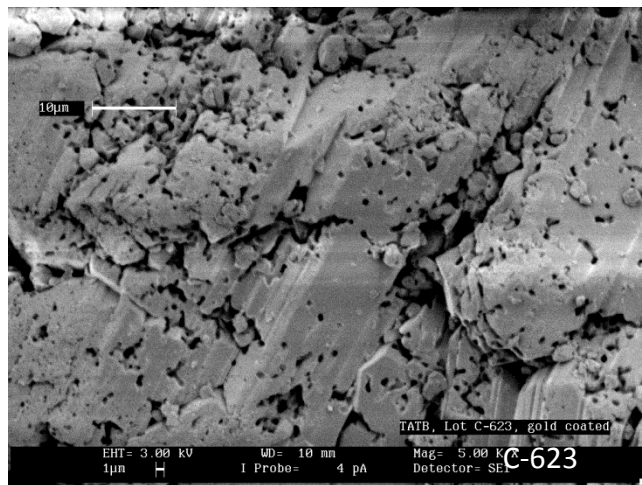
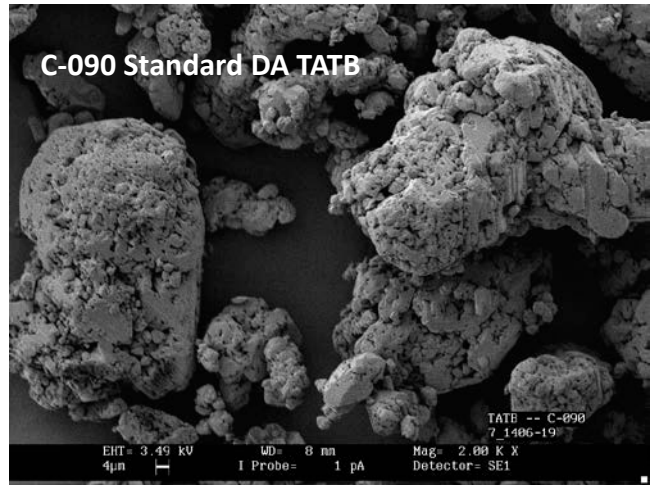
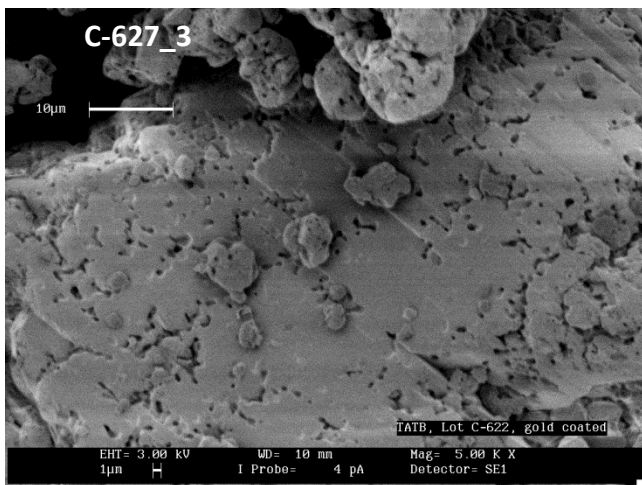
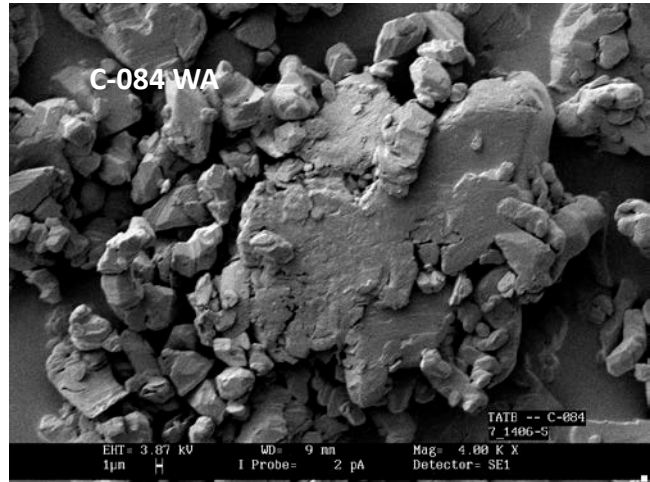
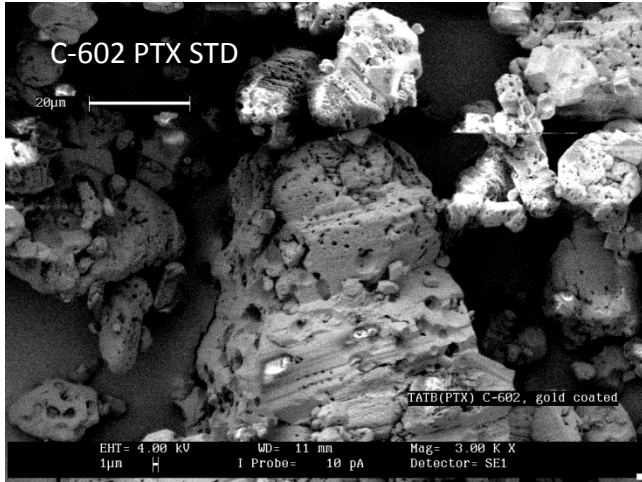


Figure 3b. SEMs of two legacy samples of DA TATB (C-602 and C-090), an ATK pilot batch (C-627_3) and a BAE pilot batch (C623) all show “worm hole” structure from the ammonium chloride removal process compared to WA TATB (C-084) in which such “worm holes” are notably absent.

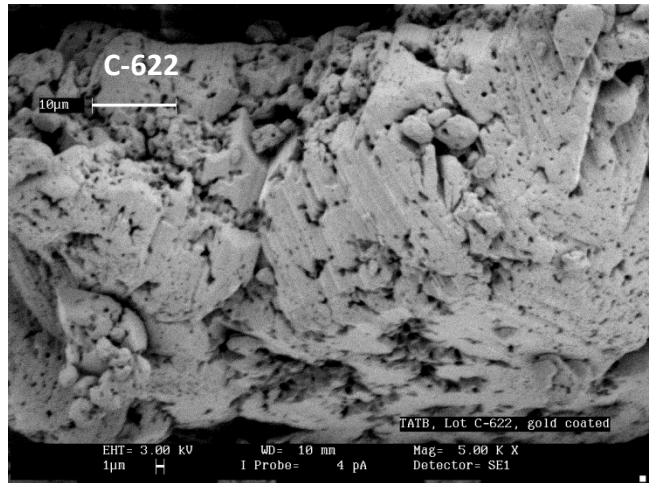
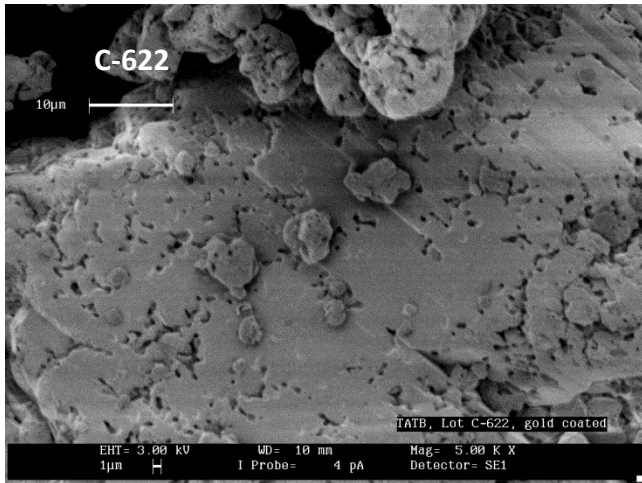
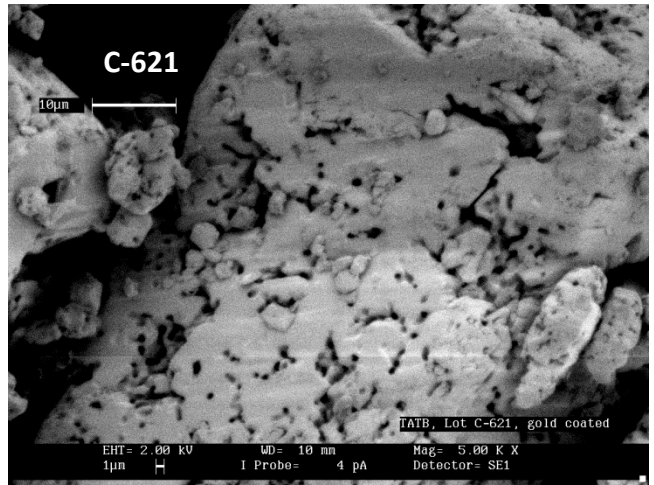
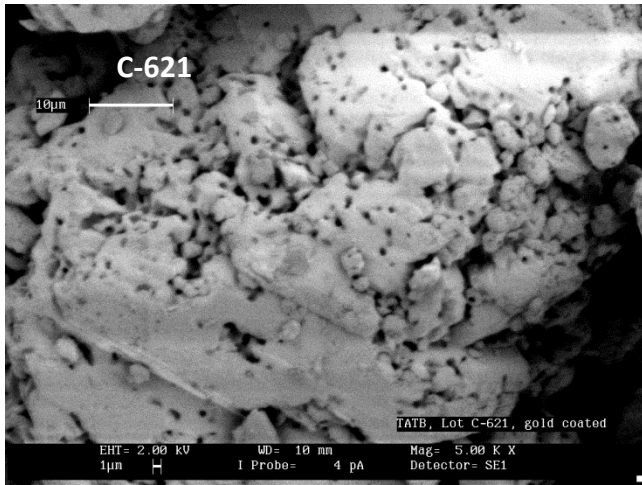
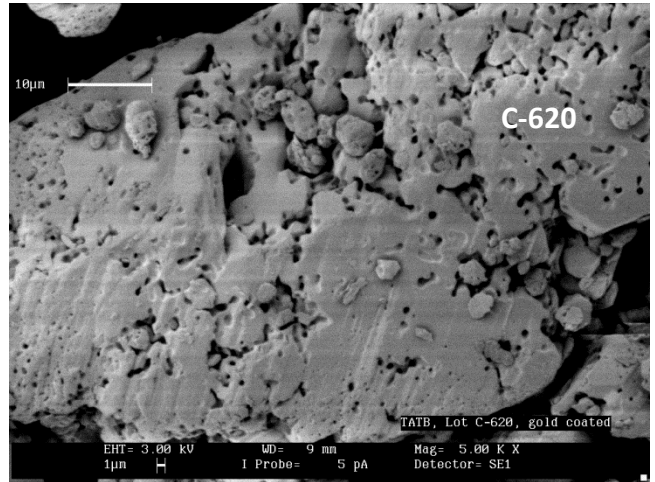
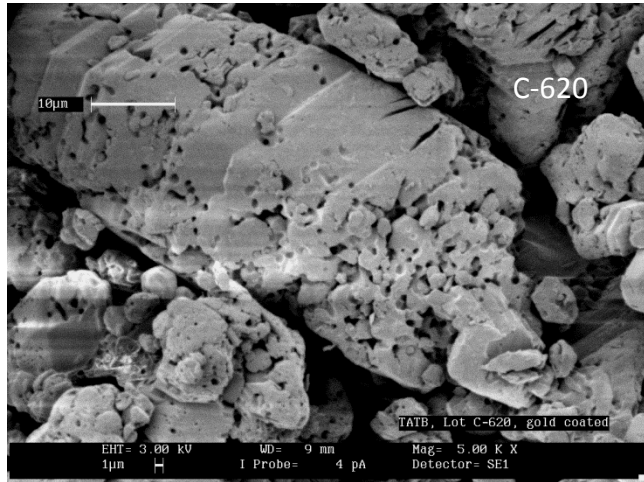


Figure 3c. SEMs from 3 of the 4 BAE pilot lots all showed “worm holes” to different extents.

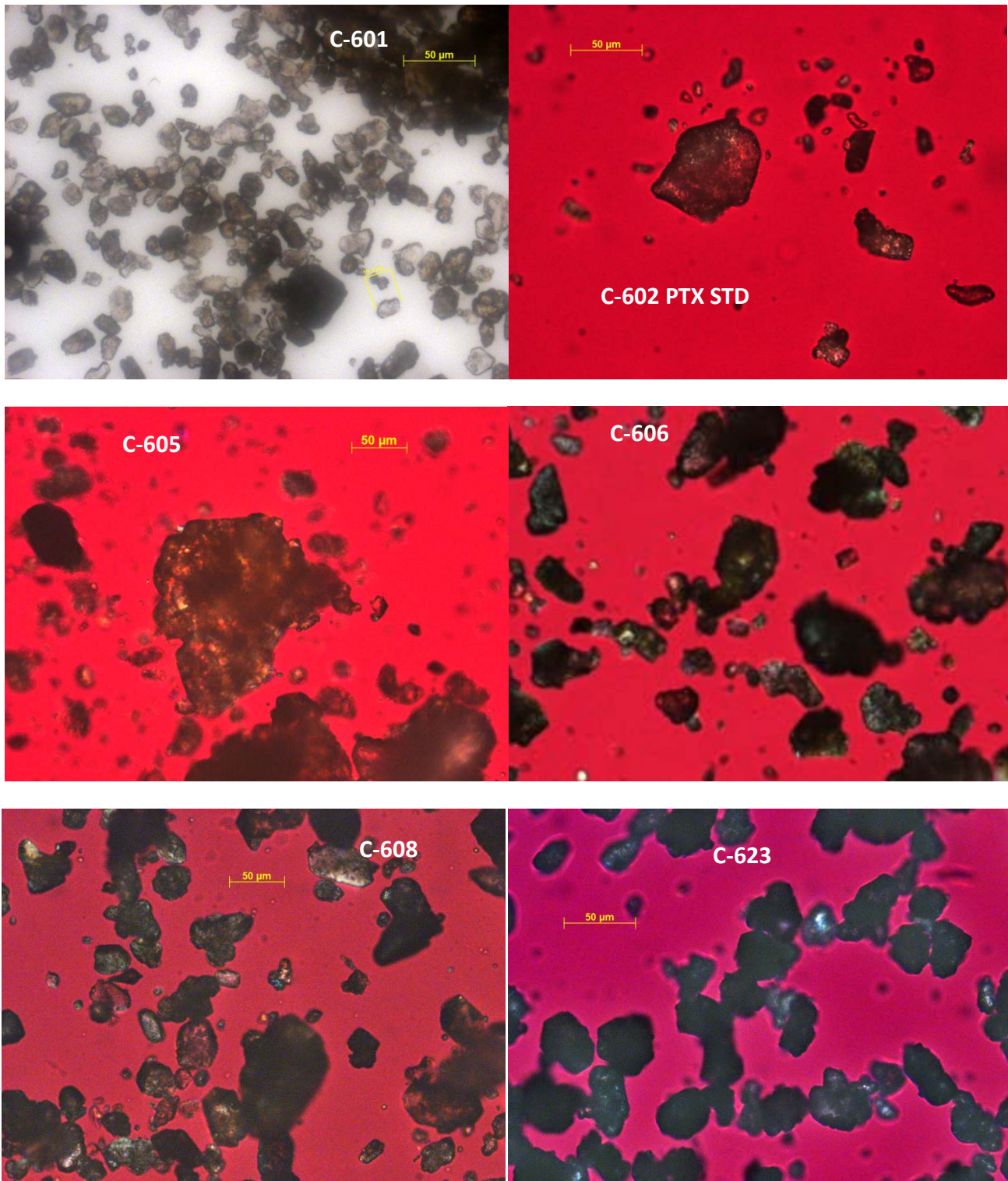


Figure4a. Polarized light micrographs of lab scale DA TATBs show relatively poor crystal quality, i.e., light is not transmitted through them uniformly and internal defects are often visible. The ATK sample (C-601) looks remarkably good.

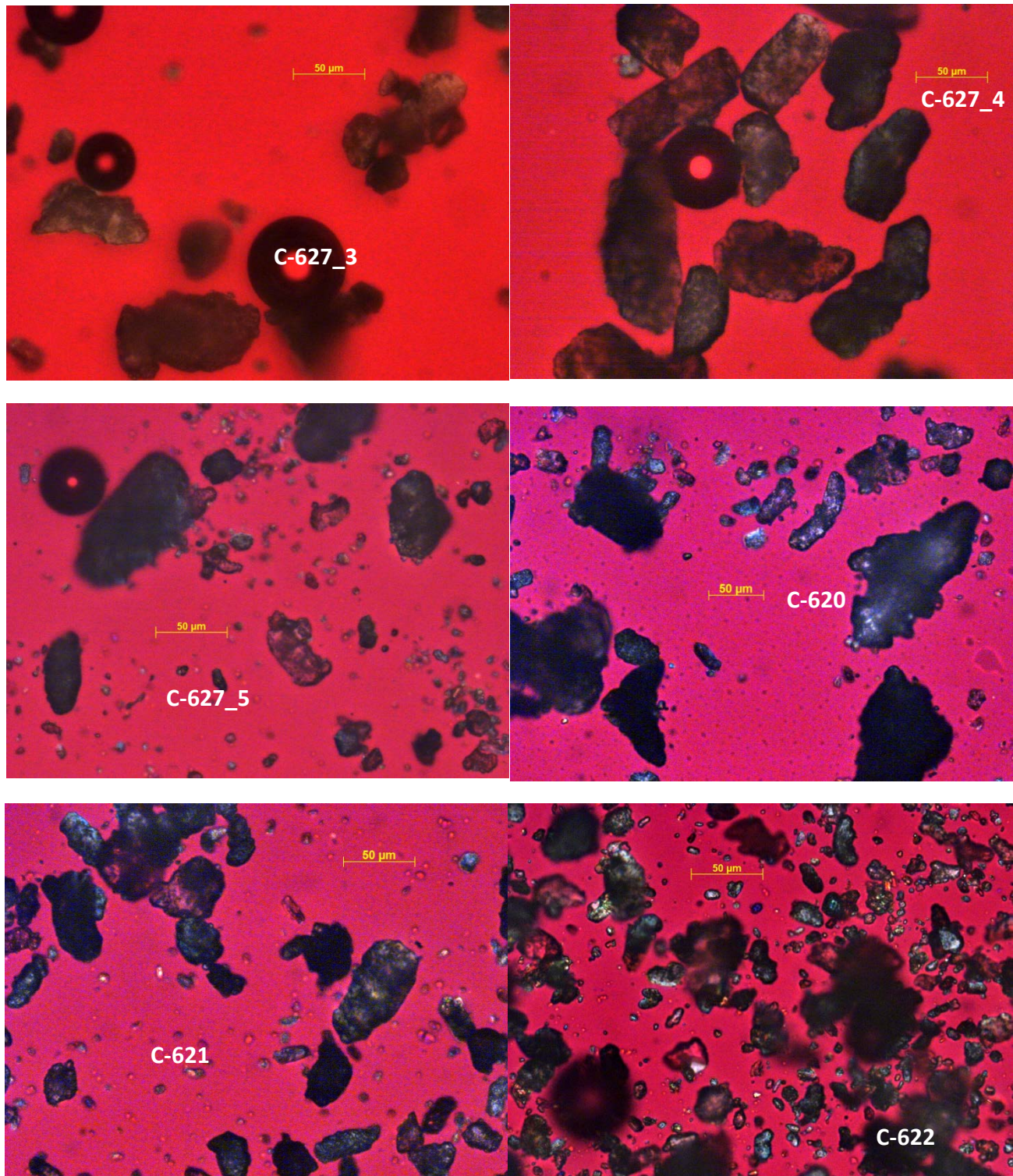


Figure 4b. Polarized light micrographs of Pilot scale TATB was similar to lab scale. Note the lack of fines and larger crystals in ATK's C-627_4 batch.

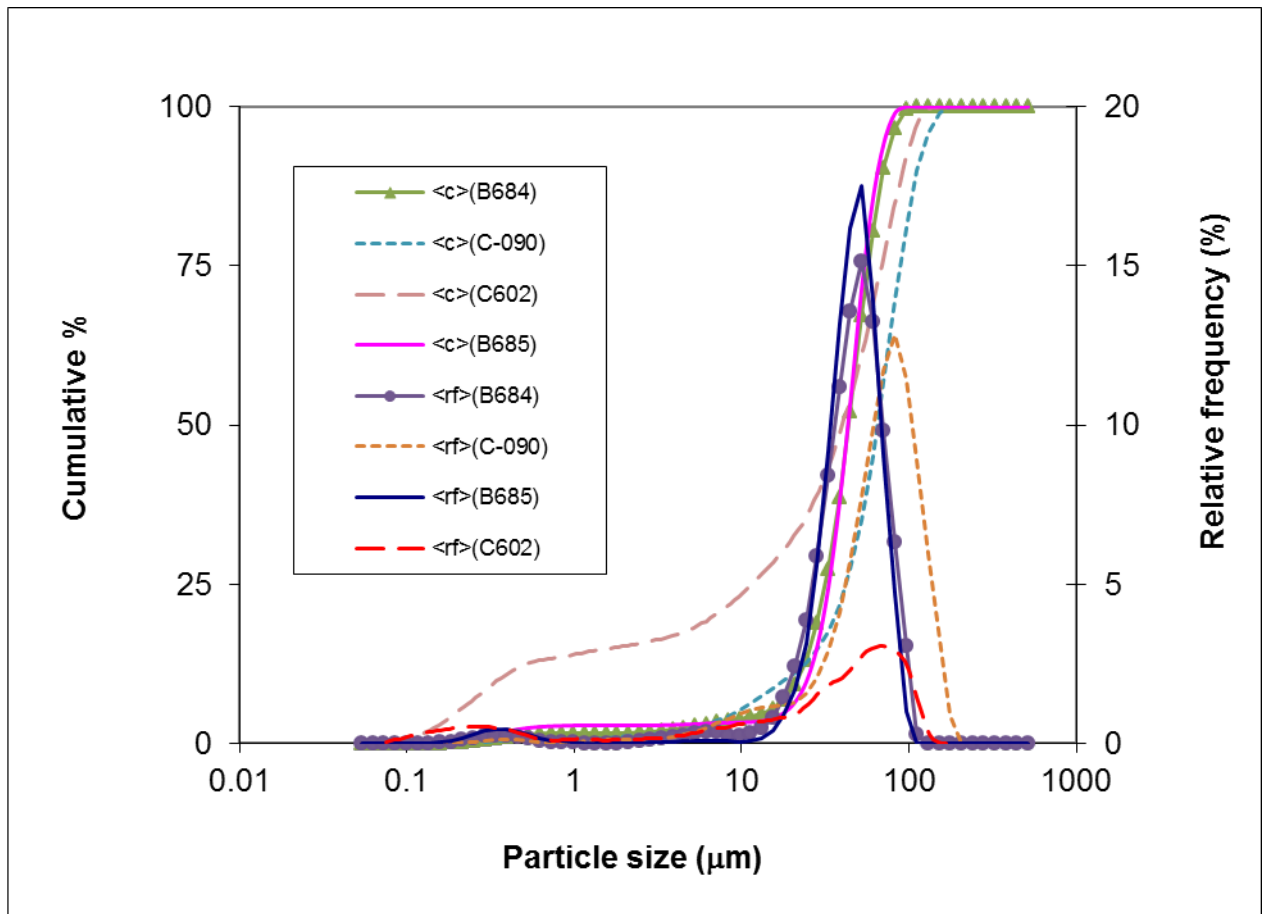


Figure 5a. DA TATB from 3 legacy lots synthesized by the original 3 different manufacturers shows some variability between manufacturers. There is also a significant sensitivity difference between the Micromeritic and the Malvern particle size results with respect to the number of fines.

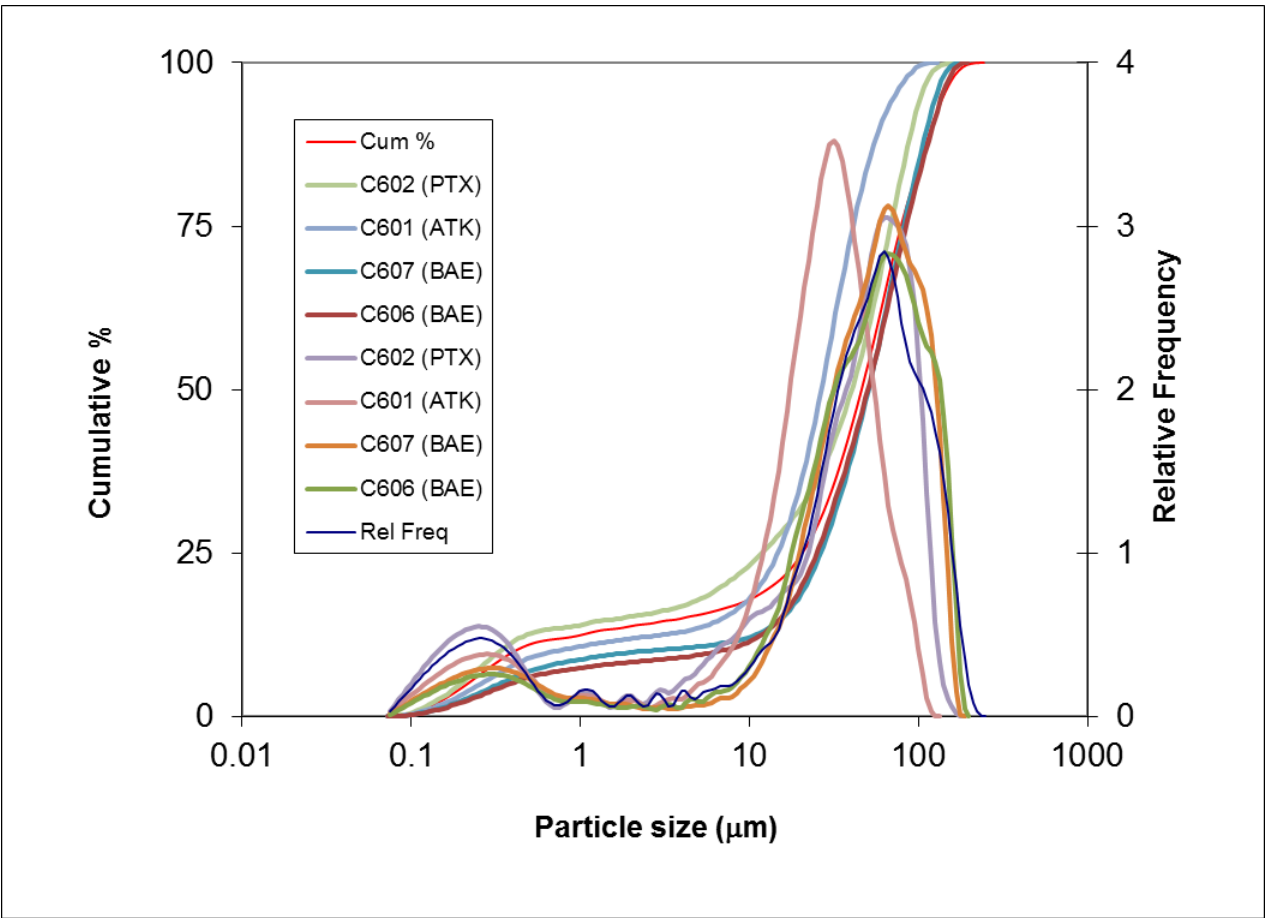


Figure 5b. Particle size distributions from DOTC TATB lab scale samples were similar to legacy DA TATB.

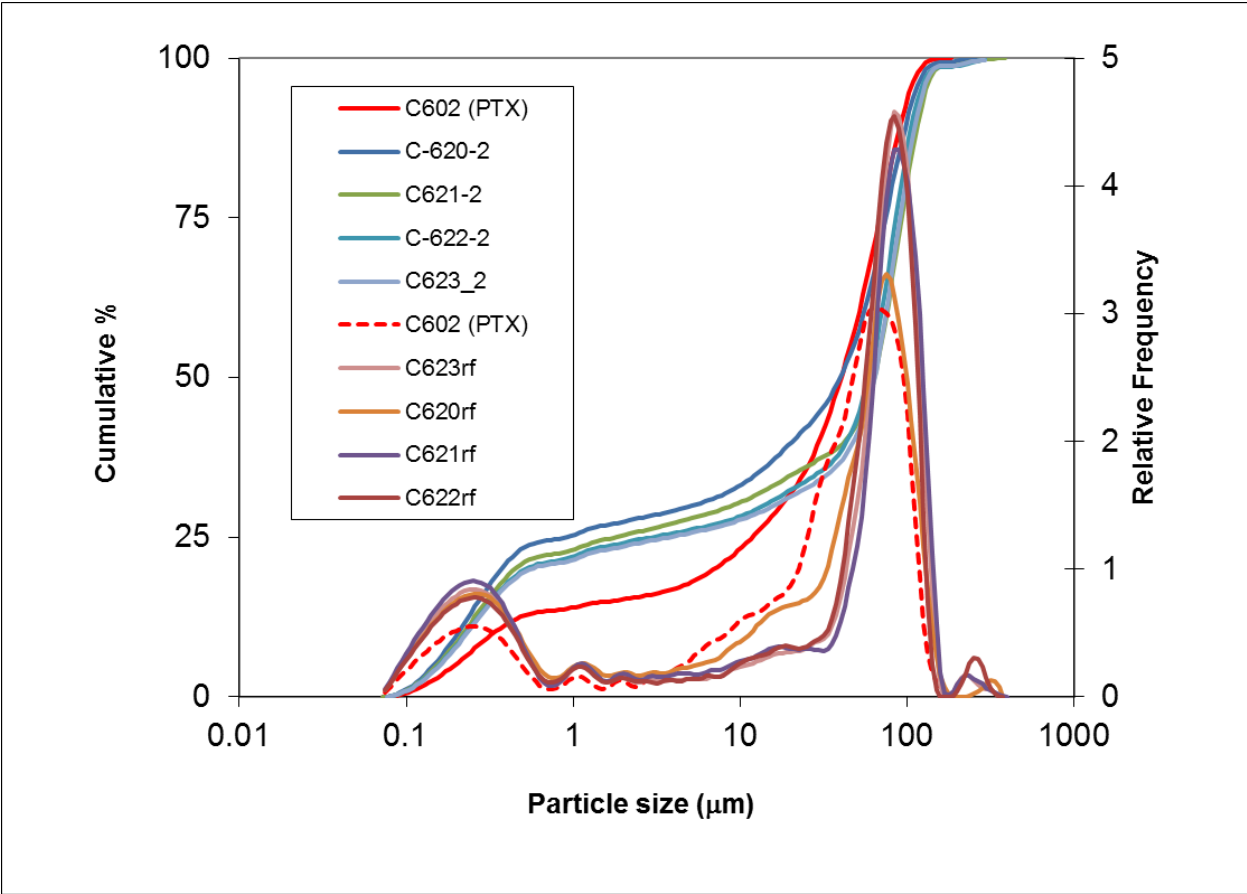


Figure 5c. Particle size distributions from DOTC BAE pilot scale TATB samples showed more fines than the Pantex legacy DA TATB.

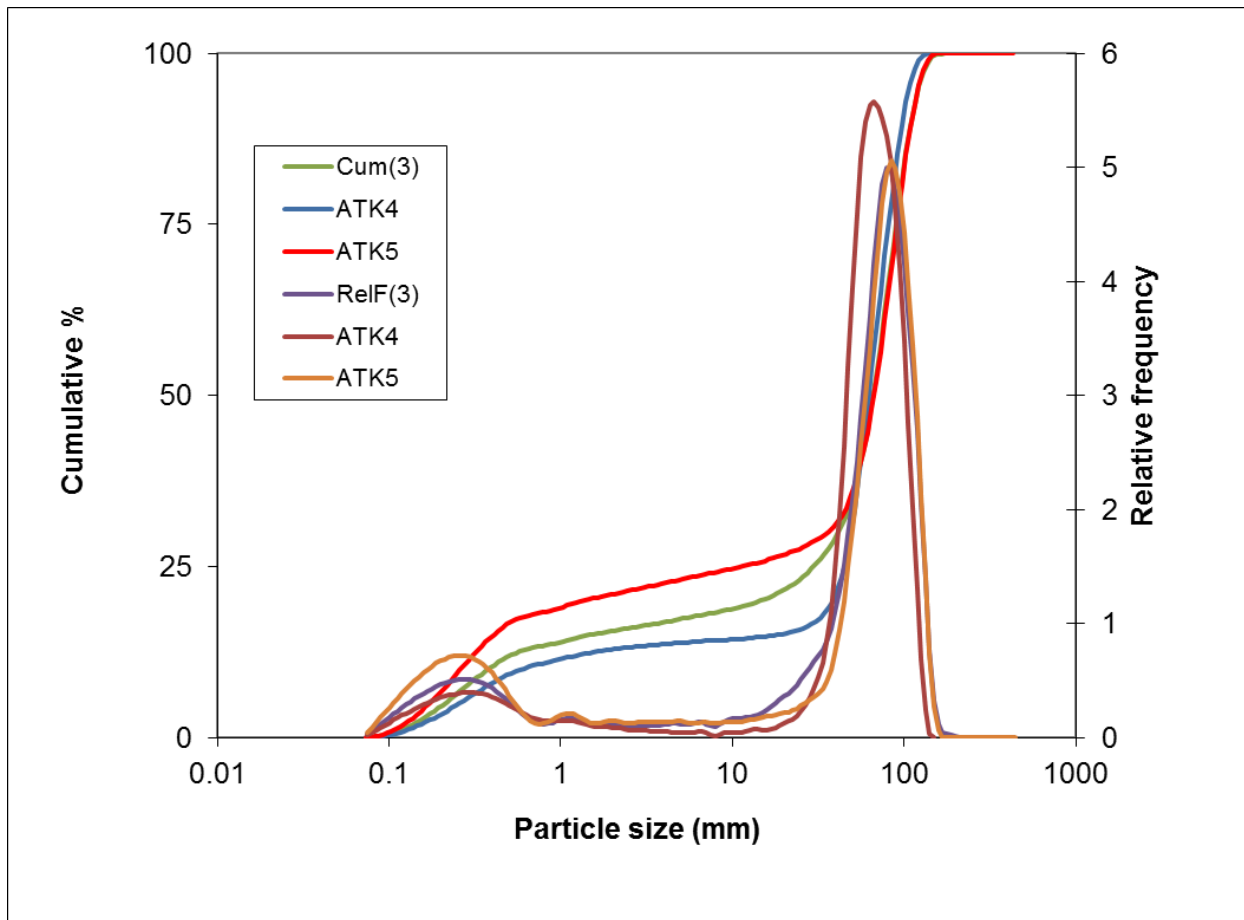


Figure 5d. Particle size distributions from DOTC ATK pilot scale TATB samples showed varying degrees of fines, but typically more than the Pantex legacy DA TATB.

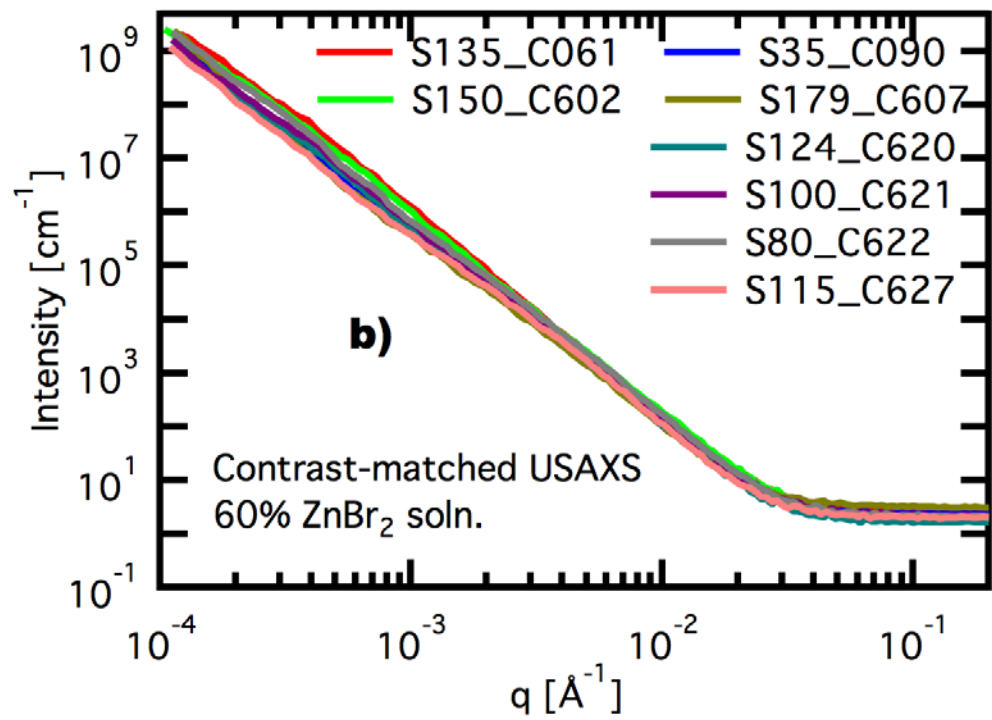
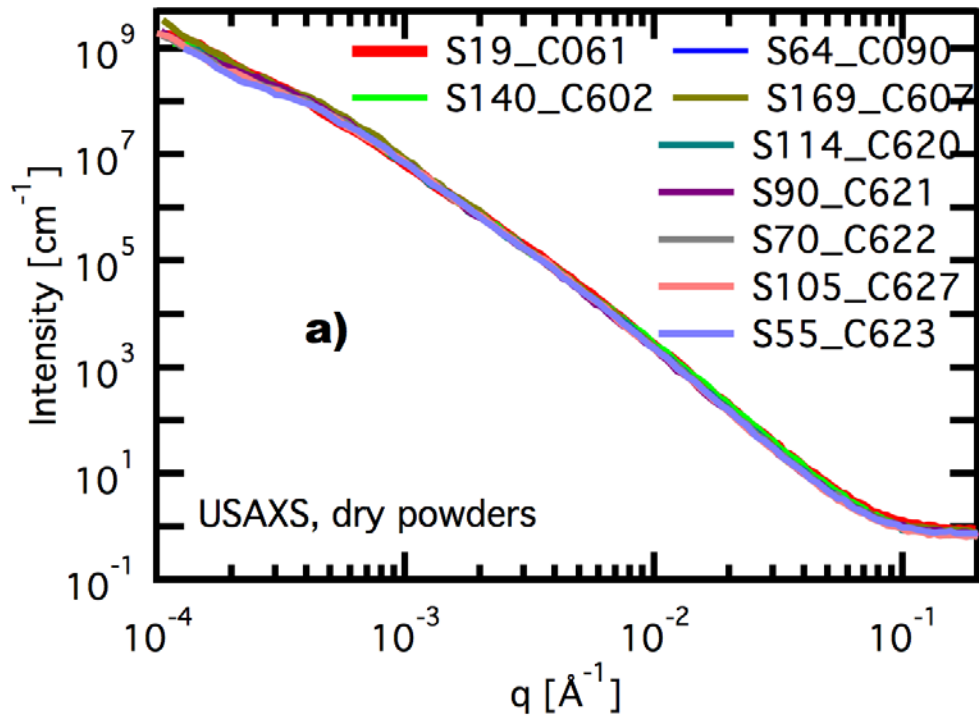


Figure 6. Comparison of legacy DA (C-090) with lab and pilot scale TATBs from BAE and ATK showed void content was similar, implying crystal quality was comparable.

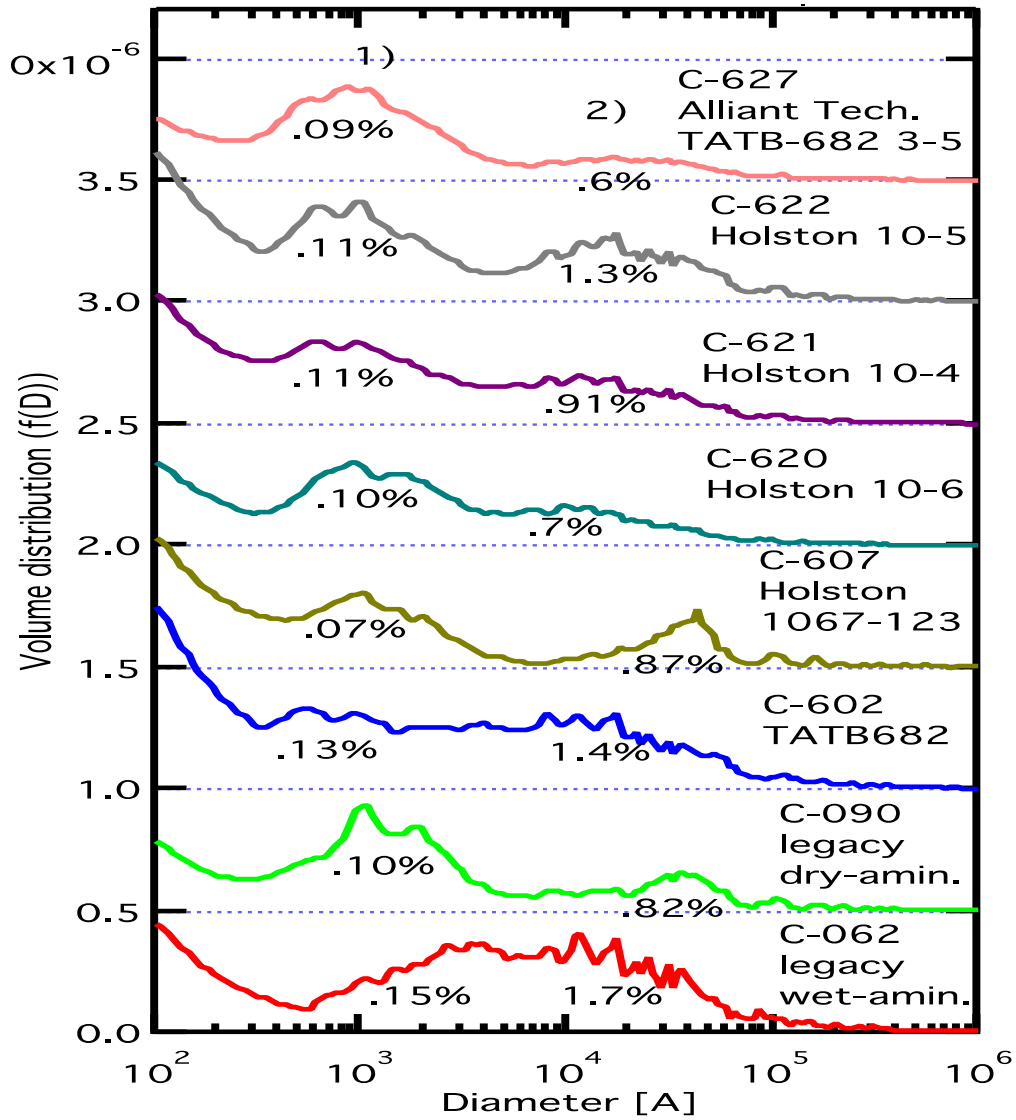


Figure 7: Void distributions derived from the contrast-matched USAXS. Dry-aminated TATB generally has scatterers ~ 100 nm that occupy $\sim 0.1\%$ of the volume; this peak is marked 1) The distributions at larger sizes 2) likely have contributions from structures not necessarily associated with internal voids.

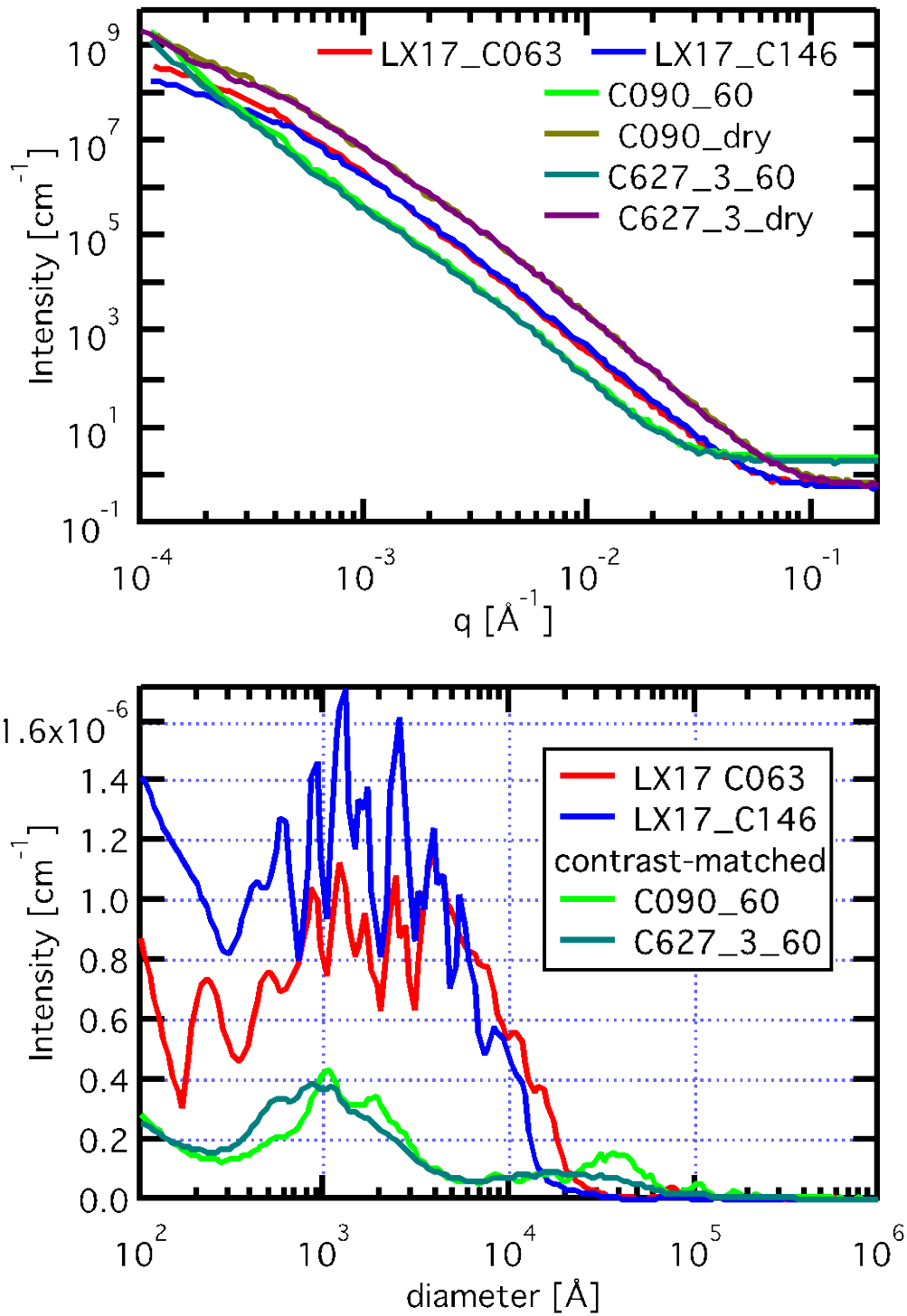


Figure 8: USAXS of TATB powders, LX-17, and TATB in contrast-matched ZnBr₂ solutions, top pane. The lower pane is the derived size distributions from the LX-17 samples and contrast-matched TATB, and plotted on the same axes, indicate the approximate intracrystalline void contribution to overall LX-17 porosity distribution.

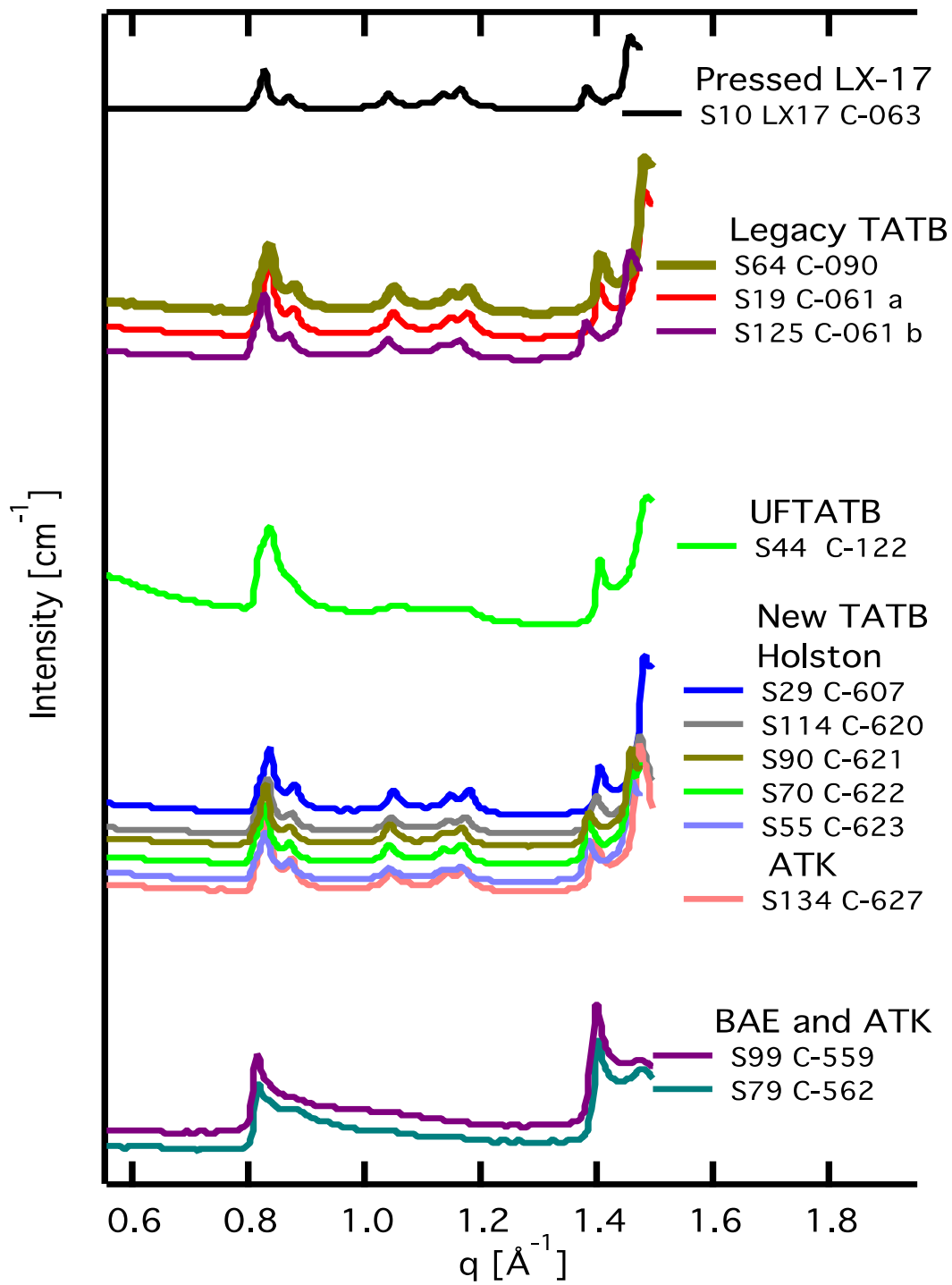


Figure 9: small to wide angle x-ray scattering of various lots of TATB. Lots formed via the Benzinger process (Legacy and New TATB groupings) exhibit similar molecular diffraction

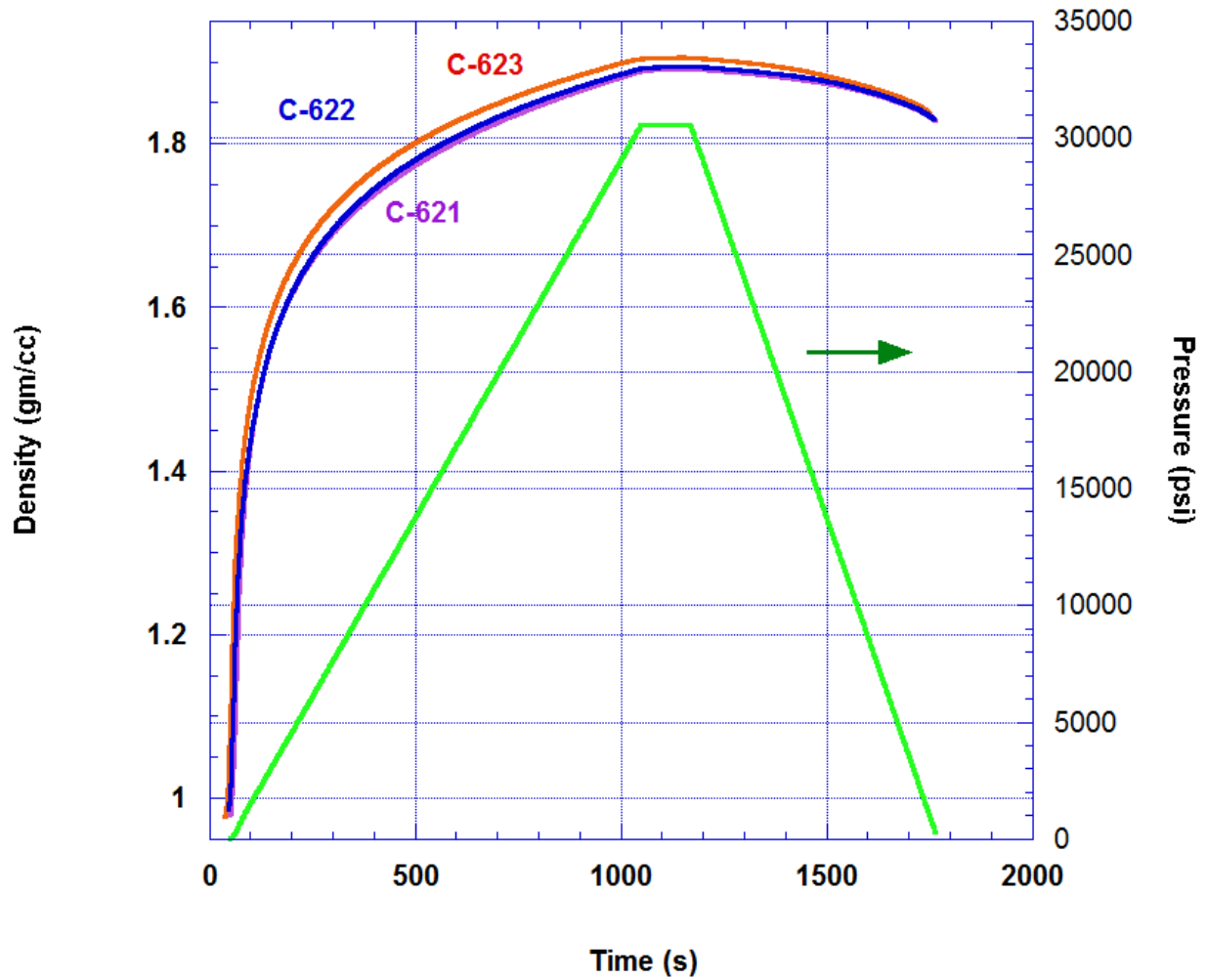


Figure 10. Typical compaction plots show the density and pressure but not much difference is observed between different lots of DA TATB.

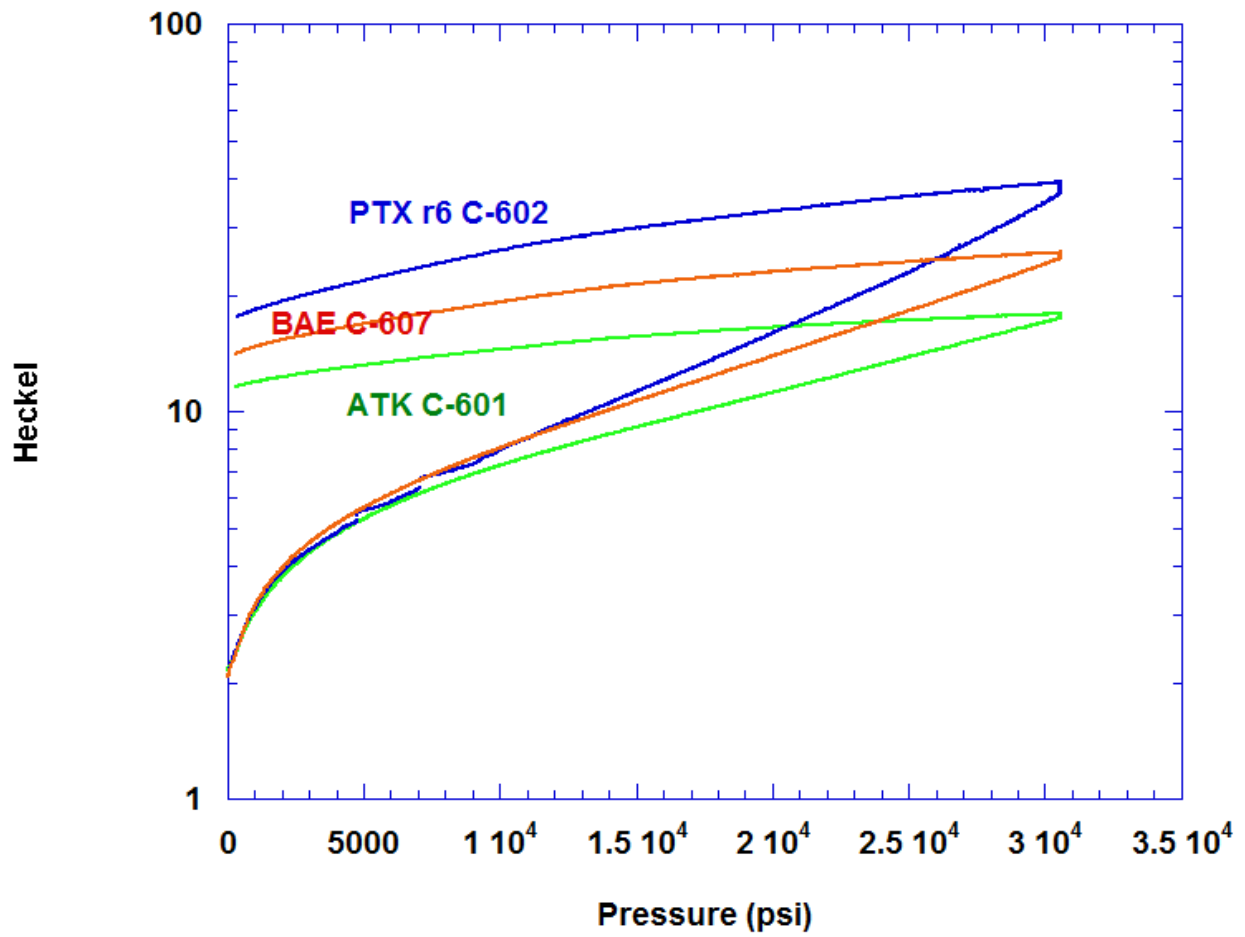


Figure 11a. Replotting the curves using the Heckle equation showed that the lab scale TATB the most easily compacted was the legacy TATB, followed by BAE while ATK was harder.

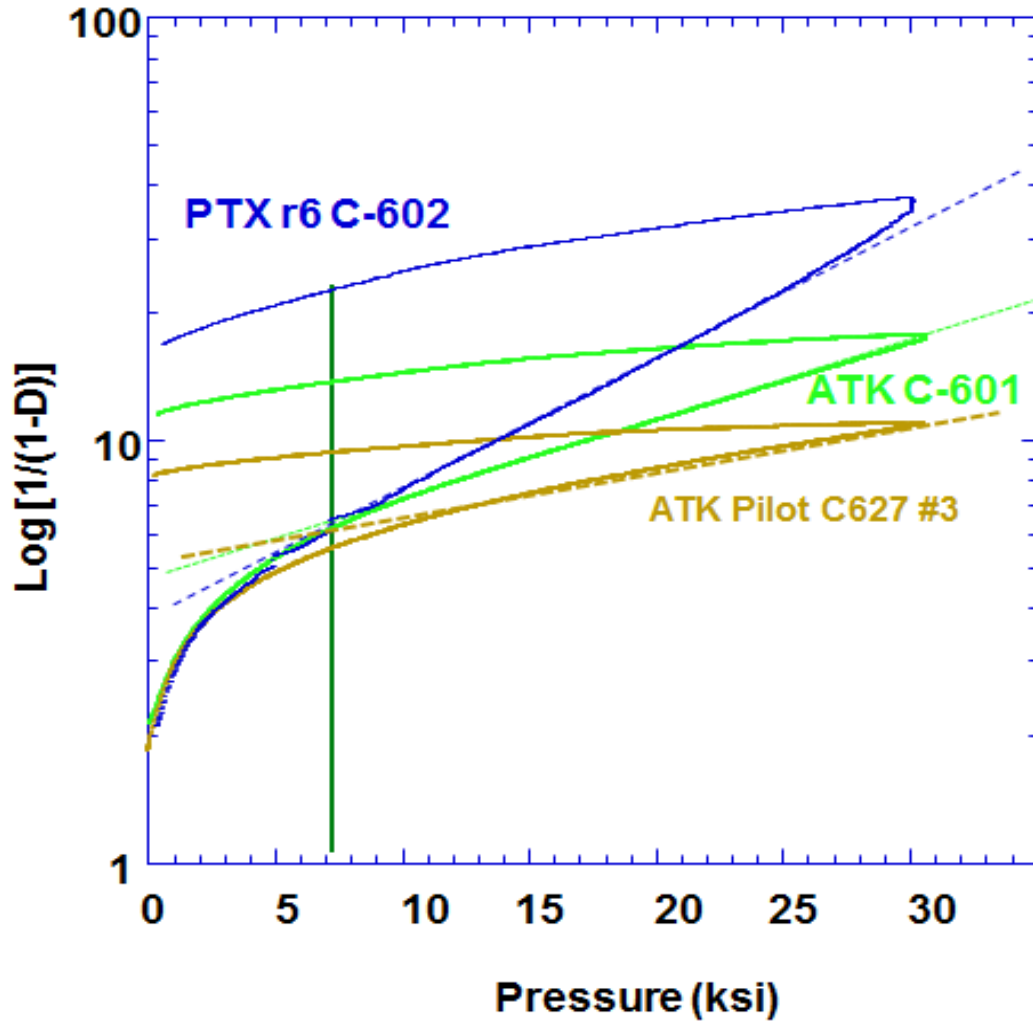


Figure 11b. Comparison of ATK samples from lab and pilot with legacy material show that they tend to be “harder” than the Pantex Standard DA TATB.

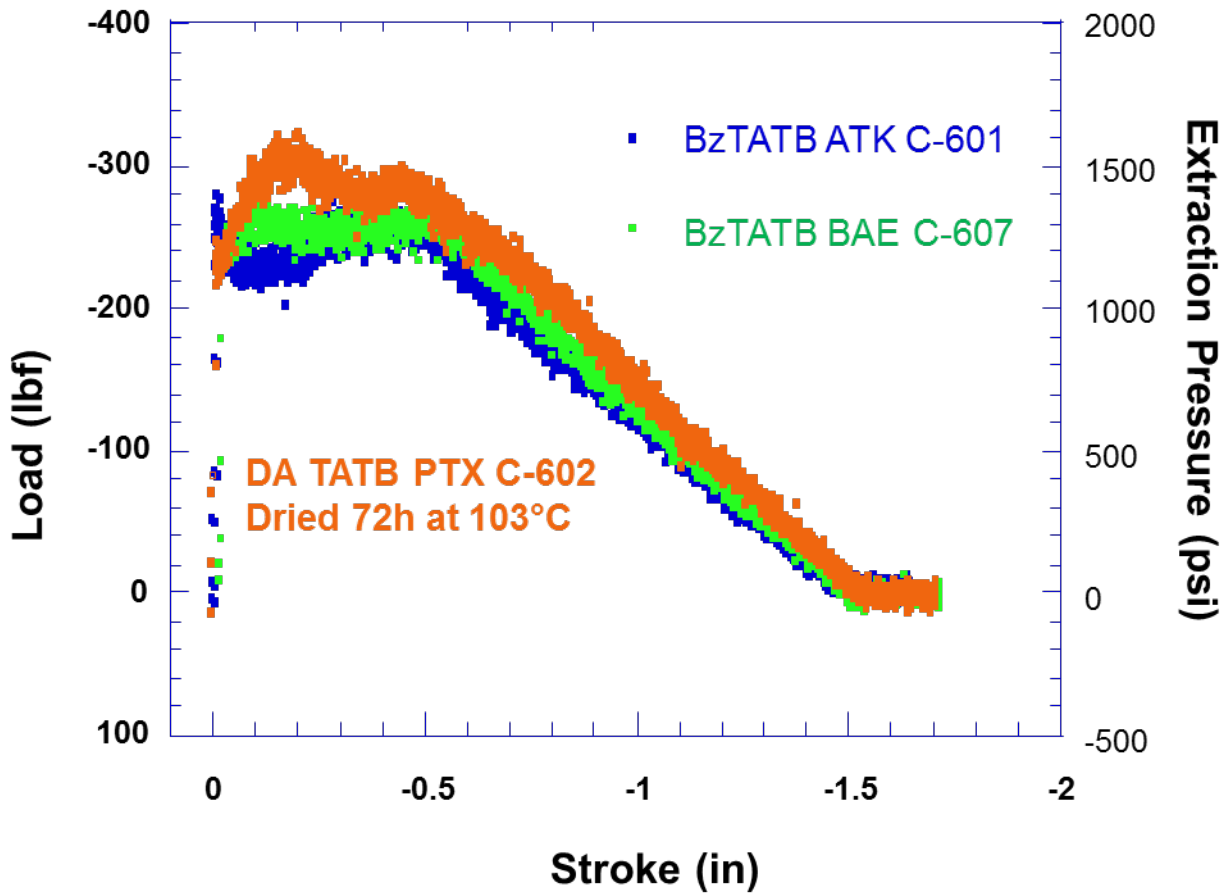
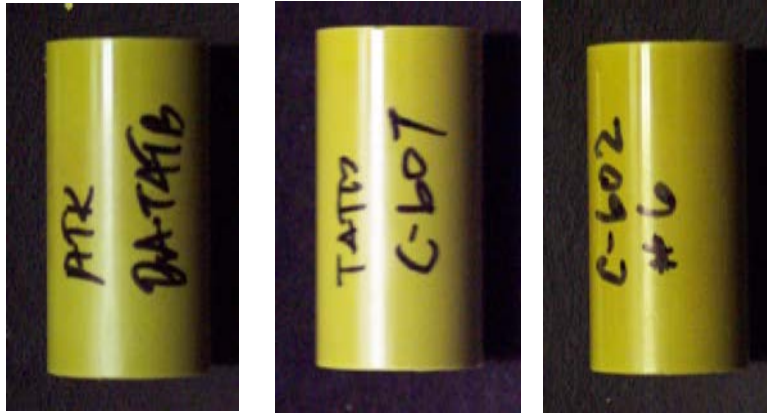


Figure 12a. Extraction force versus position in the die for the above samples shows a relatively constant value until the part begins to exit the die for the new BAE and ATK DA TATBs with the standard PTX TATB only slightly higher.

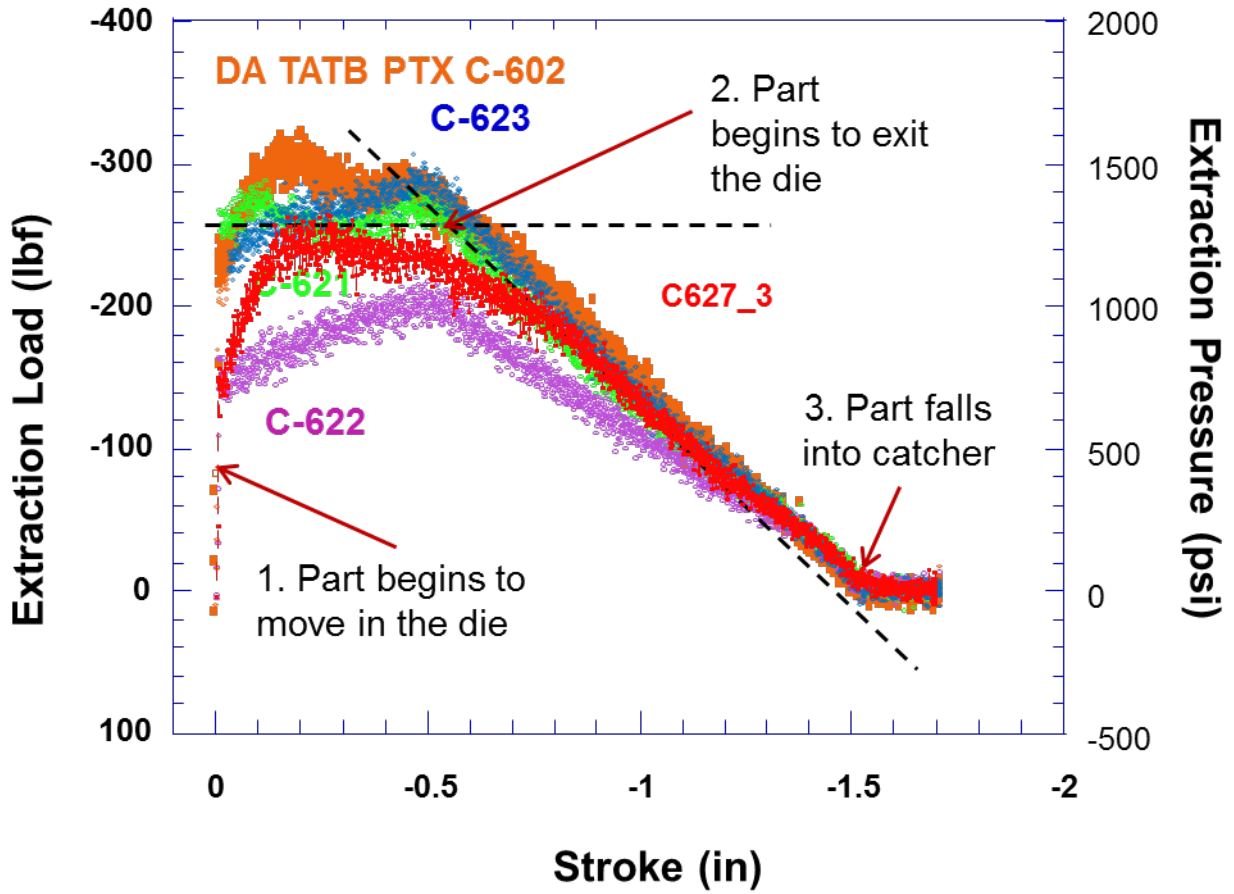


Figure 12b. Force required to extract new pilot scale BAE DA TATB was equivalent or lower than legacy DA TATB compared

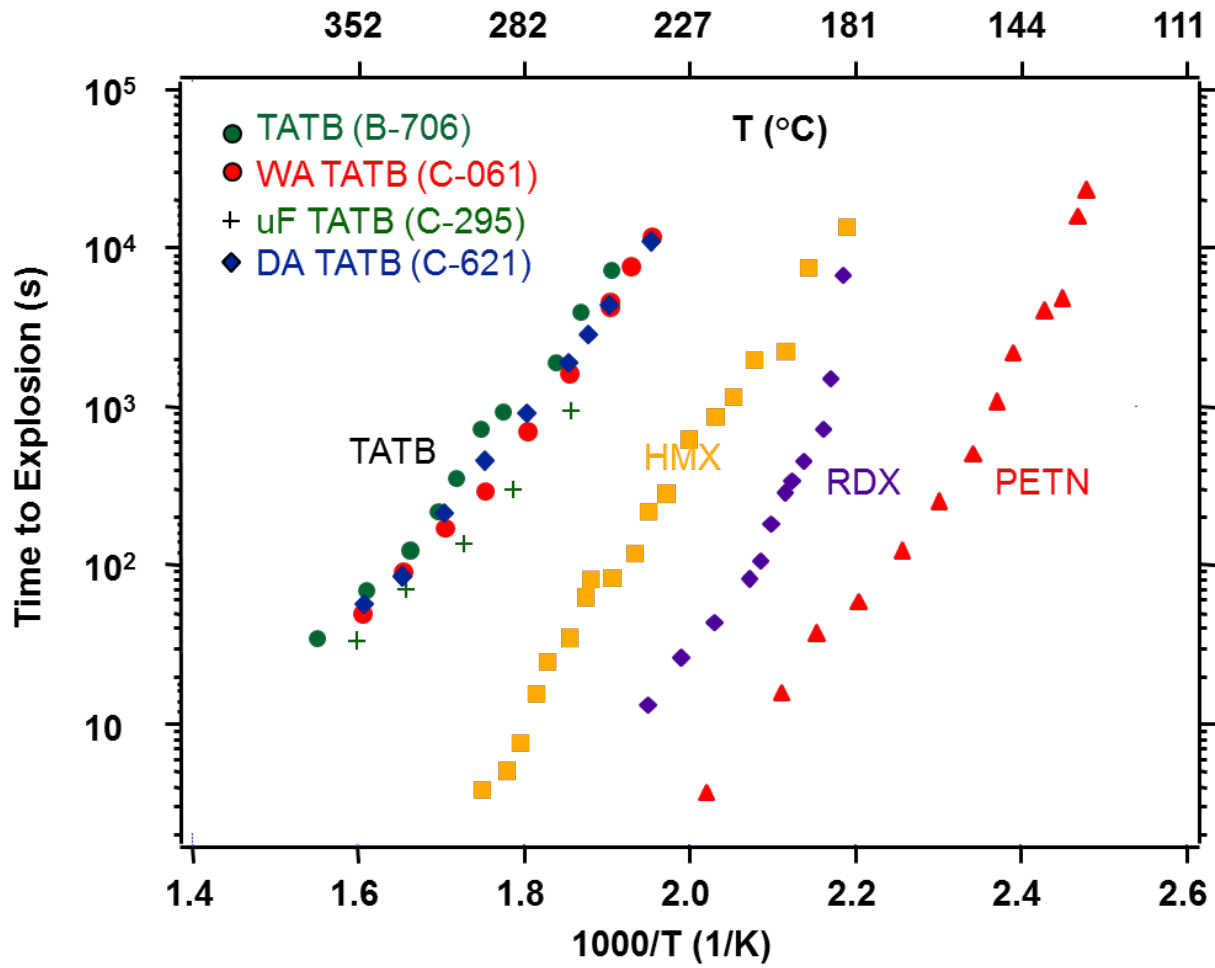


Figure 13. This ODTX plot shows several legacy TATB compared to the new BAE DA TATB from one of the pilot runs. The results are reasonably similar.



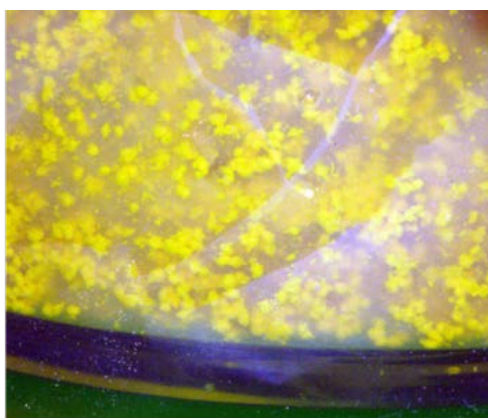
Setup: (1) Holston reactor, (2) Air motor, (3) Aspirator, (4) Vacuum trap, (5) Heater hoses



TATB suspended in Water during Initial mixing



PBX-9502 beads cooled with water after solvent phase driven off



Two phase Slurry solution prior to evaporating ethyl acetate



Beads filtered using Buchner funnel ready for drying in the oven



RM-03-H series molding powder

Figure 14. The 50 gram slurry coater used at LLNL to make PBX-9502 formulation from DOTC TATBs using approximately the same process used with legacy PBX-9502 produced reasonable molding powder (example shown is an LX-17 like formulation but PBX-9502 results were similar).

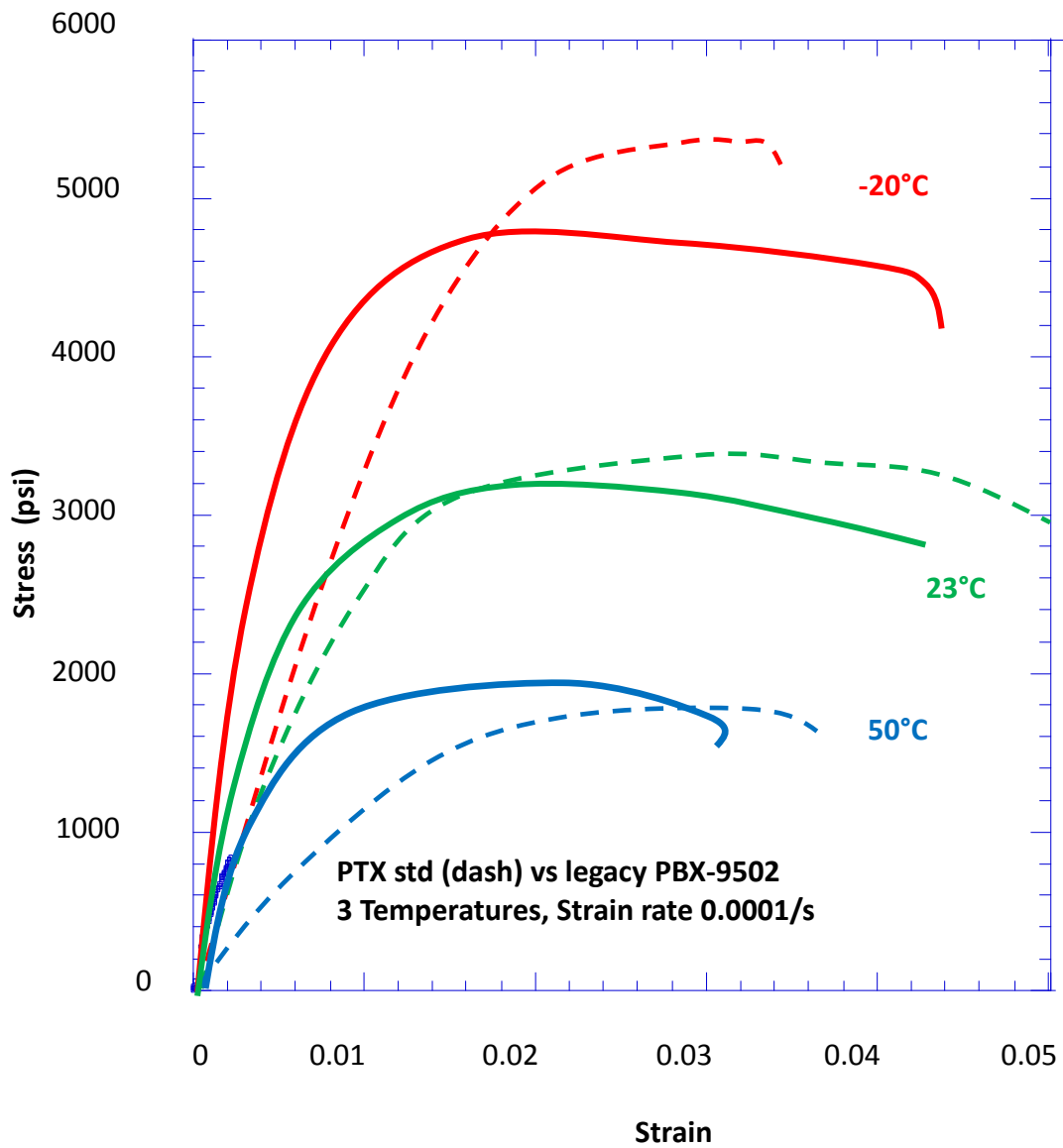


Figure 15a. Comparison of 50 gram formulation of PBX-9502 from the DA TATB Pantex standard (dashed) and legacy PBX-9502 (solid lines) show fairly dramatic differences in modulus and strength.

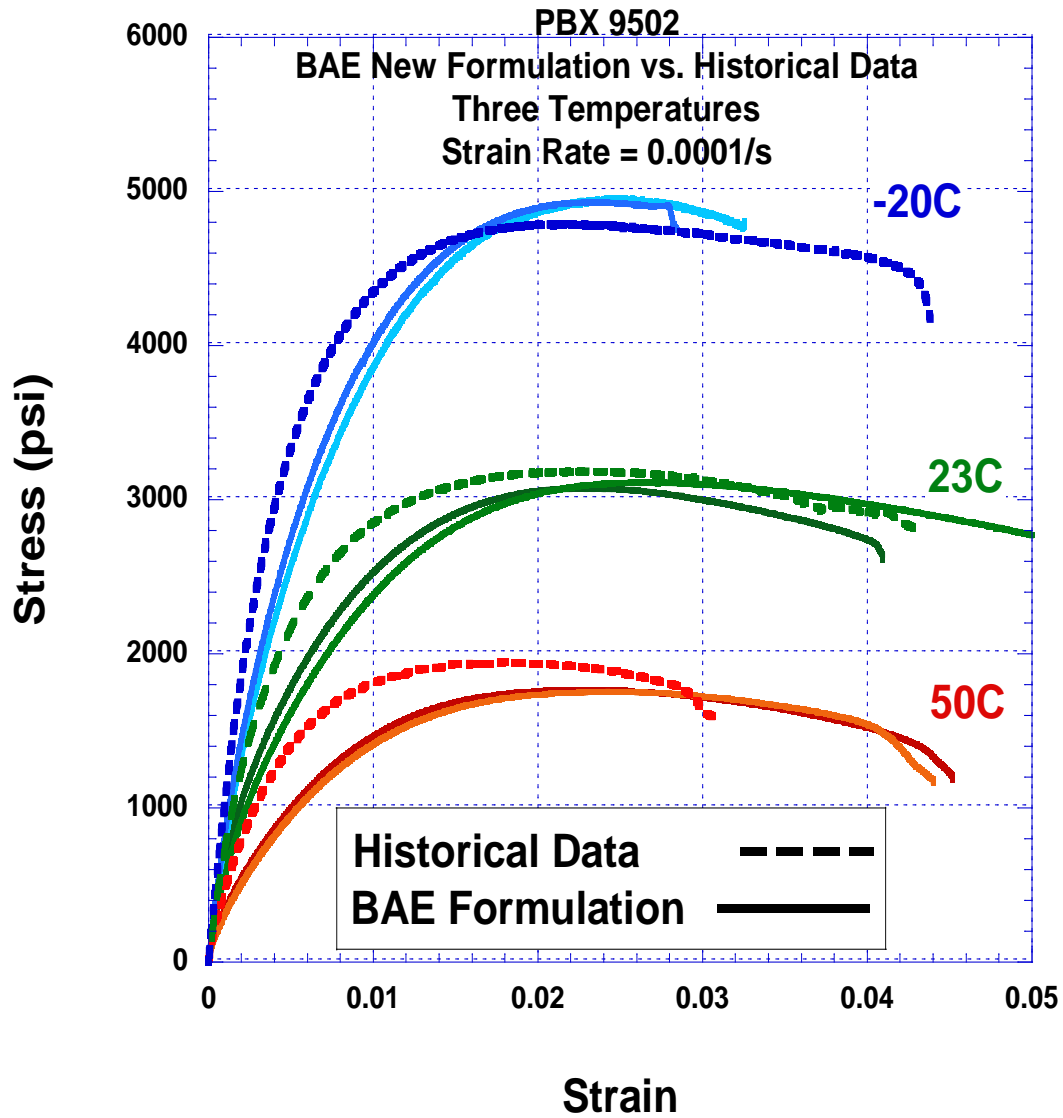


Figure15b . PBX-9502 formulated from BAE pilot lot C-620 were lower modulus but similar in strength compared to compressive properties of historical PBX-9502 samples. This is possibly associated with levels of fines and/or incomplete crystallization of the binder in the new formulations.

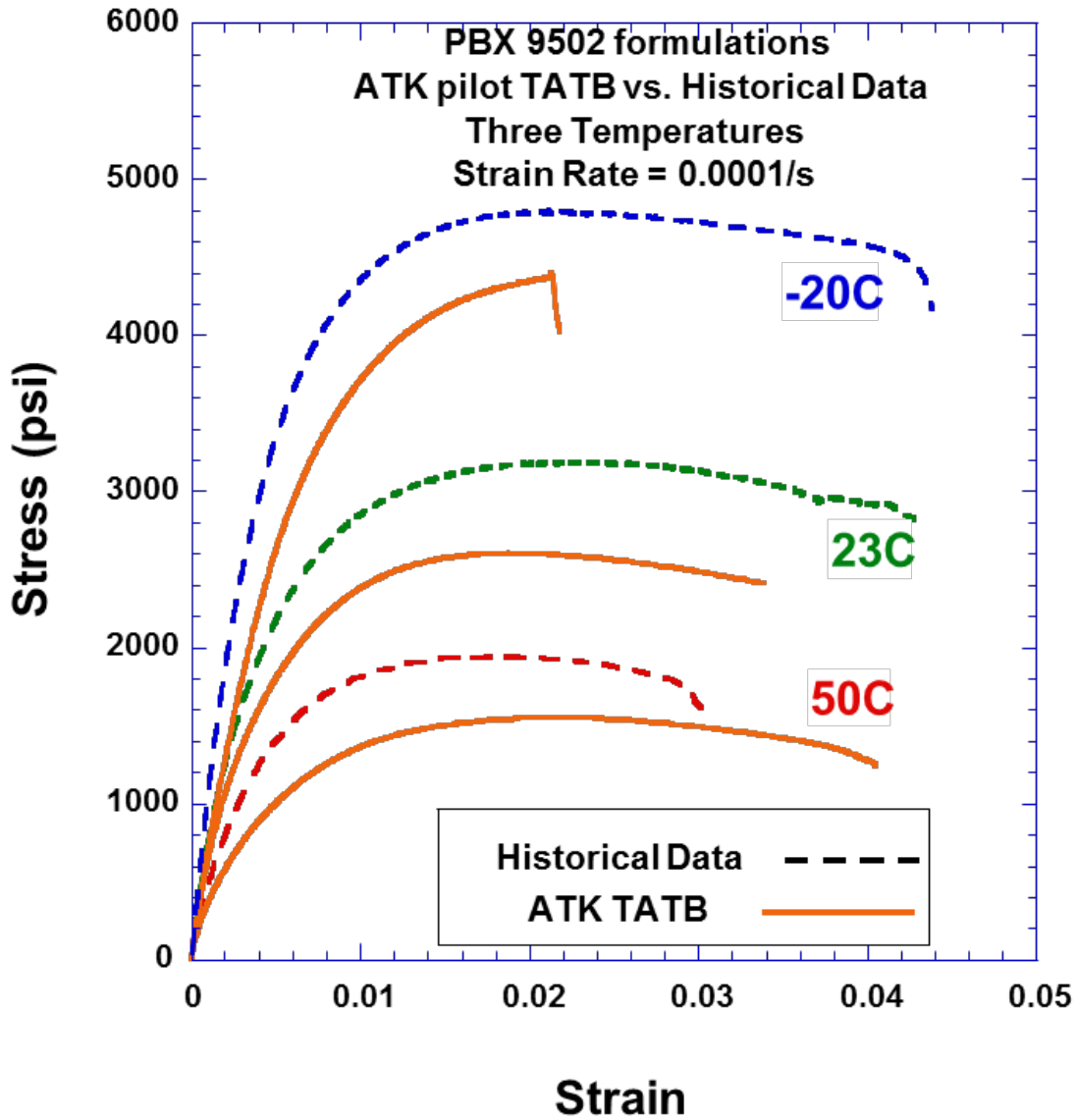


Figure 15c. PBX-9502 formulated from ATK pilot lot C-627-3 showed lower modulus and strength than historical PBX-9502 samples probably because the FK 800 binder has not yet completely crystallized in the new PBX-9502 formulation.

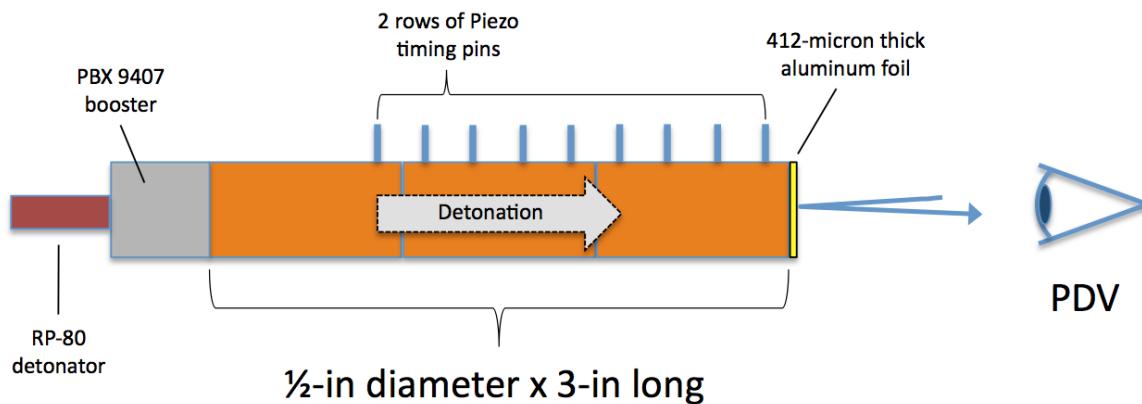
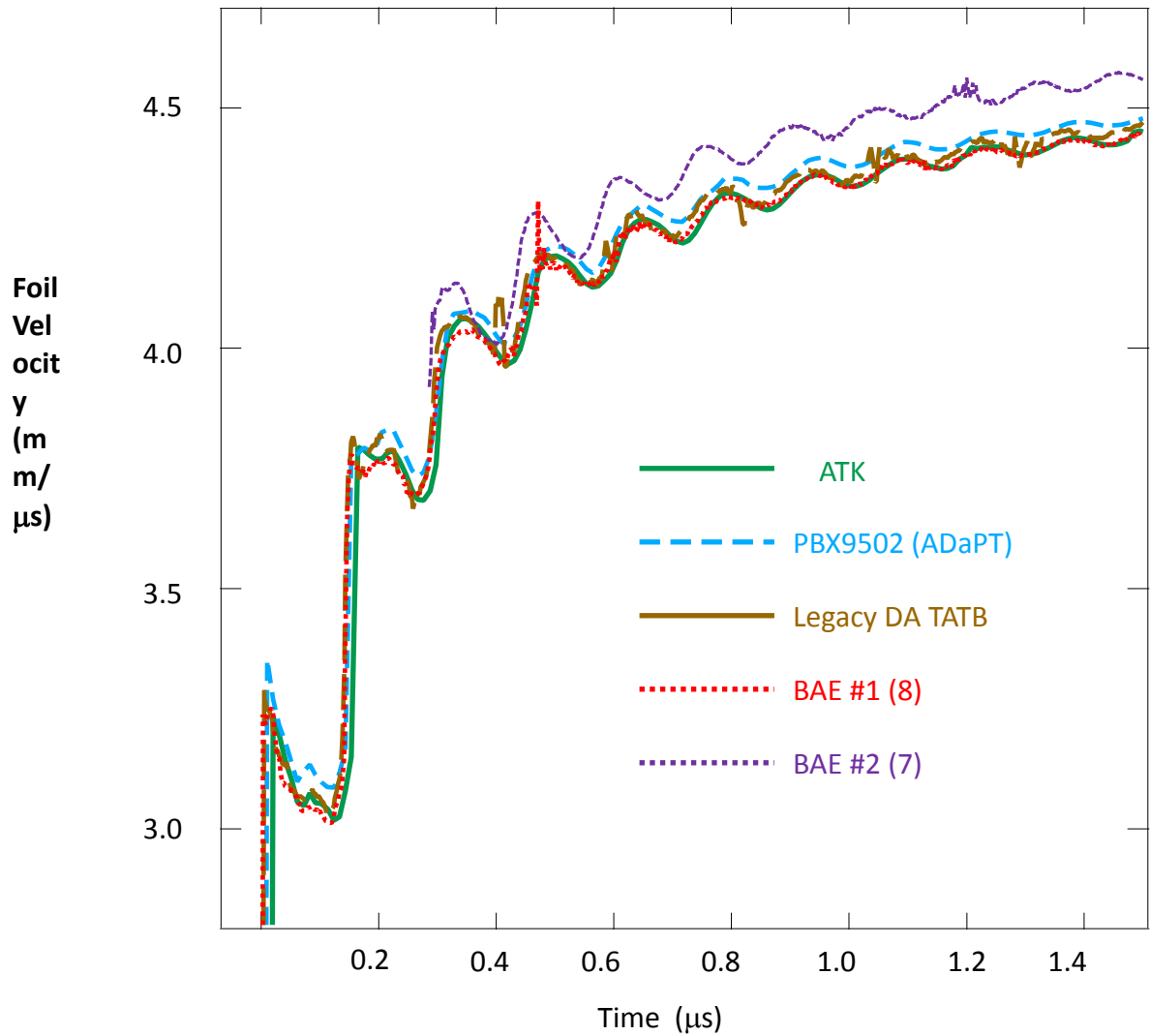


Figure 16. Foil surface velocity measurements versus time for small PDV rate sticks of PBX-9502-like explosive from BAE (C-620) pilot scale and PX (C-602) legacy and ATK (C627_3) DA TATB fall close to legacy ADaPT PBX-9502 (above). A schematic of the test is shown below.